NASA TECHNICAL NOTE

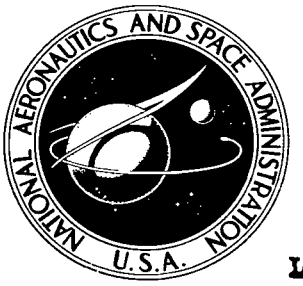

NASA TN D-6063

BOUNDARY-LAYER TRANSITION STUDY OF SEVERAL POINTED BODIES OF REVOLUTION AT SUPERSONIC SPEEDS

by William A. Cassels and James F. Campbell

Langley Research Center
Hampton, Va. 23365

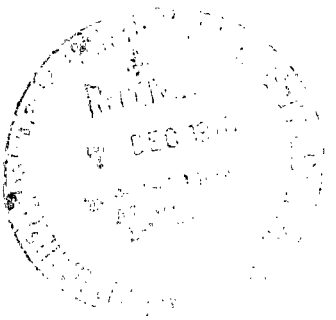

NATIONAL AERONAUTICS AND SPACE ADMINISTRATION • WASHINGTON, D. C. • NOVEMBER 1970

1. Report No.	2. Government Accession No.	3. Recipient's Catalog No.
NASA TN D-6063		

4. Title and Subtitle	5. Report Date
BOUNDARY-LAYER TRANSITION STUDY OF SEVERAL POINTED BODIES OF REVOLUTION AT SUPERSONIC SPEEDS	November 1970
	6. Performing Organization Code

7. Author(s)	8. Performing Organization Report No.
William A. Cassels and James F. Campbell	L-7159
	10. Work Unit No.
9. Performing Organization Name and Address	720-01-11-02
NASA Langley Research Center Hampton, Va. 23365	11. Contract or Grant No.
	13. Type of Report and Period Covered
12. Sponsoring Agency Name and Address	Technical Note
National Aeronautics and Space Administration Washington, D.C. 20546	14. Sponsoring Agency Code

15. Supplementary Notes

16. Abstract

Boundary-layer transition by the sublimation and impact-pressure techniques and force tests have been performed on three Haack-Adams bodies of revolution of fineness ratios 7, 10, and 13 at zero angle of attack for free-stream Mach numbers of 2.00, 2.75, and 4.63 and a range of Reynolds numbers based on model length of 6 to 15×10^6 with and without a roughness strip. The grit method of inducing turbulence was found to provide for a nearly complete turbulent flow over the models at the lower Mach numbers and higher Reynolds numbers considered in this study while the amount of trip drag was less than 8 percent of the model drag with transition fixed. A method of interpreting sublimation data was discussed and used and the results compared well with the impact-pressure results.

17. Key Words (Suggested by Author(s))	18. Distribution Statement
Transition Bodies of revolution Flow visualization Supersonic flow	Unclassified – Unlimited

19. Security Classif. (of this report)	20. Security Classif. (of this page)	21. No. of Pages	22. Price*
Unclassified	Unclassified	67	$3.00

*For sale by the Clearinghouse for Federal Scientific and Technical Information
Springfield, Virginia 22151

BOUNDARY-LAYER TRANSITION STUDY OF SEVERAL POINTED BODIES OF REVOLUTION AT SUPERSONIC SPEEDS

By William A. Cassels and James F. Campbell
Langley Research Center

SUMMARY

Boundary-layer transition by the sublimation and impact-pressure techniques and force tests have been performed on three Haack-Adams bodies of revolution of fineness ratios 7, 10, and 13 at zero angle of attack for free-stream Mach numbers of 2.00, 2.75, and 4.63 and a range of Reynolds numbers based on model length of 6×10^6 to 15×10^6 with and without a roughness strip. From the resulting data the roughness strip method of inducing turbulence was examined, sublimation-data interpretation and correlation of sublimation and impact pressure data were examined and force data were presented.

The grit method of inducing turbulence was found to provide for a nearly complete turbulent flow over the models at the lower Mach numbers and higher Reynolds numbers considered in this study while the amount of trip drag was less than 8 percent of the model drag with transition fixed. A method of interpreting sublimation data was discussed and used and the results compared well with the impact pressure results.

INTRODUCTION

The flow of boundary-layer air over the surface of an aerodynamic configuration gives rise to an important problem in wind-tunnel research and flight evaluation. In order to extrapolate wind-tunnel data to full-scale conditions, it is necessary to correct the data for the difference in skin friction between the model at low Reynolds numbers and the full-scale model at high Reynolds numbers. Hence, when extrapolating wind-tunnel model results to full-scale conditions, the transition position must be known in order to calculate the skin friction on the wind-tunnel model. Transition is usually fixed on the model by means of small grit particles placed on the model surfaces. These trips can in turn lead to undesirable drag increases which complicate the force analyses.

Numerous studies have been made concerning this boundary-layer problem associated with wind-tunnel testing and analysis (refs. 1 through 15, for example). These studies have generally been made with flat-plate and cone configurations. The present investigation is conducted on contoured bodies of revolution. Specifically, this study considers the boundary-layer characteristics of three Haack-Adams bodies of revolution of fineness ratio 7, 10, and 13, respectively, at free-stream Mach numbers from 2.0

to 4.63 and over a Reynolds number range from 6×10^6 to 15×10^6 based on model length. The location of transition from laminar to turbulent flow for the bodies of revolution and range of tests conditions was determined by two methods; namely, by impact-pressure measurements along the model surfaces, and by observations of the sublimation of a chemical material sprayed on the models. Both of these methods of locating transition were investigated with and without the use of grit particles to induce turbulent flow artificially. The objectives of the present study were as follows:

(1) To examine the "grit" method of inducing transition to turbulent flow, including the effectiveness and drag of the trip.

(2) To study the usefulness of sublimation techniques in locating the transition region on bodies of revolution, using impact-pressure data as a reference.

SYMBOLS

A	cross section area
$C_{D,o}$	drag coefficient at zero angle of attack
c_f	local skin-friction coefficient
d	diameter of model
h	sublimation chemical coating thickness
K_1, K_2, K_3	constants
k	roughness height
l	model length
M	Mach number
M_c	sublimation chemical coating molecular weight
p	static pressure

p_t impact or stagnation pressure

p_v sublimation chemical coating vapor pressure

R_k roughness Reynolds number, $\frac{u_k k}{\nu_k}$

R_k' roughness Reynolds number with Mach number adjustment, $R_k\left[1.11\left(1 + \frac{\gamma - 1}{2} M_k^2\right)\right]^{0.5+\omega}$

$R_{l,\infty}$ free-stream Reynolds number based on length of model

R_u universal gas constant

$R_{x,k}$ Reynolds number at roughness strip, $\frac{u_\delta x_k}{\nu_\delta}$

r model radius

T absolute static temperature

T_t absolute total temperature

t time required for sublimation chemical to sublimate

u velocity in x-direction

x distance along longitudinal axis of body; measured from model nose

x_{sub} distance from model nose to painted-sublimation border along longitudinal axis of model

y distance in radial direction measured from body surface

γ ratio of specific heats

δ total boundary-layer thickness

ρ_c	sublimation chemical coating density
ν	kinematic viscosity
ω	exponent of viscosity-temperature relation

Subscripts:

2	conditions downstream of normal shock wave
b	beginning of transition as defined at local minimum impact pressure
base	base of model
e	end of transition defined at local maximum impact pressure
k	conditions at roughness strip
m	point of maximum impact pressure slope in transition region
max	maximum
s	determined from sublimation test
surf	conditions on surface of model
t	total
tr	transition region
δ	conditions at the outer edge of boundary layer
∞	conditions in free stream

TESTS AND APPARATUS

Tunnel Description

All tests were performed in the low and high Mach number test sections of the Langley Unitary Plan wind tunnel which is a variable-pressure continuous-flow facility. The test sections are 1.22 meters square and 2.13 meters long. The nozzles leading to the test sections are of the asymmetric sliding block type which permits a continuous variation in Mach number from 1.5 to 2.9 in the low Mach number test section and from 2.3 to 4.7 in the high Mach number test section.

Test Conditions

The following table gives the test conditions used in this study:

$R_{l,\infty}$	T_t, °R	p_t, atm	T_t, °R	p_t, atm	T_t, °R	p_t, atm
	$M_\infty = 2.00$		$M_\infty = 2.75$		$M_\infty = 4.63$	
6×10^6	610	0.626	610	0.916	635	2.492
9	610	.939	610	1.373	635	3.738
12	610	1.252	610	1.831	635	4.984
15	610	1.565	610	2.290	635	6.230

Models

The three models used in this study are sting-mounted Haack-Adams bodies of revolution with fineness ratios of 7, 10, and 13. (See ref. 16.) It should be noted that these bodies are minimum wave drag configurations for boattail bodies with a given length, volume, and base area. Each model has an afterbody closure ratio (A_{base}/A_{max}) of 0.532 and an overall length of 91.44 cm (3 ft). The following table gives the critical dimensions of each model and figure 1 gives the longitudinal distribution of body radii for the three models. This table and figure 1 together describe the dimensions of each model used. The actual coordinates of the three models may be found in reference 17.

Model	l/d_{max}	d_{max}, cm	d_{base}, cm
A	13	7.033	5.131
B	10	9.144	6.670
C	7	13.061	9.528

Three basic types of tests were conducted: longitudinal impact-pressure tests, sublimation tests, and force-balance tests. The boundary-layer impact-pressure test involved the use of an impact probe for measuring the variation of total pressures longitudinally and several distributions vertically. Figure 2 illustrates the placement and shape of the impact probes for this test. For the impact-pressure tests an electrical contact was used to show when the probe was touching the model ($y = 0$). Then the probe was retracted a measured amount for each reading. The models were moved forward and rearward in the tunnel to obtain the longitudinal distributions.

The sublimation test utilized a chemical which sublimates faster in turbulent than in laminar flow due to the higher shear stress present in turbulent flow. Through a time sequence of photographs of the model with a clock in the background the position of the transition region could be determined by the pattern of the painted and sublimated areas. The force-balance tests measured the total drag acting on the bodies. These tests were performed on all models at zero angle of attack, which was attained by finding the orientation corresponding to zero normal force.

Tests were performed with and without grit on the model. The grit strip is a 0.32-cm wide band of carborundum grit around the body 3.05 cm ($x/l = 0.033$) from the nose. The carborundum particles were shaken through a series of sieves with grids sized so that the carborundum particles remaining on the number 60 sieve are of a certain mean diameter. A representative number of particles were measured. The average height was found to be 0.025 cm. Figure 3 illustrates the placement of the roughness strip on model B.

Instrumentation

For pressure testing a flattened impact probe of 0.0508-cm thickness was extended into the boundary layer of the model. This thickness is approximately 1/10 or less of the boundary-layer thickness. For sublimation tests with a white sublimation chemical the models were first painted with a flat black paint. The sublimation chemical used was fluorene. The characteristics of fluorene are presented in the following table from references 18 to 20:

Compound	Fluorene
Formula	$C_{13}H_{10}$
Specific gravity	1.2
Molecular weight	166.2 g/g-mole
Solvents	Benzene Freon Petroleum ether (used in this study)
Color	White
Melting point	235° F (386° K)

Drag data were obtained from force-balance tests by using a 6-component strain-gage balance. The drag was corrected to free-stream static conditions at the base.

The data from the impact-pressure and force-balance tests were output in the form of punched cards for computer-data reduction and standard printout.

RESULTS AND DISCUSSION

Impact-Pressure Tests Results

In this study, the transition region is defined as the region between the local minimum and maximum of the impact pressure distribution curve. The local minimum is identified as the start or beginning of transition from laminar to turbulent flow, and the local maximum is identified as the beginning of fully turbulent flow (end of transition). This terminology is illustrated in figure 4. Reference 5 shows that this transition-region definition is very close to the beginning and end of transition as defined by using the boundary-layer thickness. The impact-pressure data presented in figure 5 show the pressure region involving the local minimum, positive curve slope, and local maximum. This is typical in all pressure data except those curves for which this region extends off the end of the model.

Figure 5 presents sample $p_{t,2}/p_{t,2,\infty}$ distributions along the models at various heights above the model surface for some of the extremes in Mach number and Reynolds number tested with grit on and off. These data show that the characteristic trends in the transition region are consistent throughout the model boundary layer since the general shape, including location of the transition region, is approximately the same regardless of the impact probe height. It should be noted that only the pressure data near transition are plotted in figure 5 and subsequent figures, since only these data are necessary for

this study. In figures 5(e), (f), and (m) the most forward impact probe position in each of these figures shows a lower impact pressure than expected for the two higher probe positions. This drop in impact pressure may possibly be due to the roughness strip.

Figure 6 presents the impact-pressure data used in this study. Because the transition trends are consistent through the boundary layer, as shown in figure 5, the profile of only one height (0.025 cm) is shown in these figures for each set of test conditions.

Grit Effectiveness

Figure 7 is a summary plot showing the effect of grit on the transition-region location for all three models. The addition of a grit strip near the nose of model A is effective in producing nearly complete turbulence on the model for Mach 2.75. Although the presence of the grit strip results in an upstream movement of the transition region at Mach 4.63, it is not as effective as at Mach 2.75. For example, for Mach 2.75, the flow is practically all turbulent near the grit for a free-stream Reynolds number of 9×10^6; whereas for a Reynolds number of 12×10^6 at Mach 4.63, turbulent flow exists over only 75 percent of the body. The grit strip, however, does induce nearly complete turbulent flow over all the models at lower Mach numbers and higher Reynolds numbers considered in this study.

In figure 8, the results of the grit-on tests are compared with data from figure 36 of reference 5 which applies to cones using a single row of spheres for the roughness strip. The agreement is good although the present data in general are somewhat lower. Values of R_k' were obtained from the R_k values given in figures of reference 8 corrected for M_δ as given in reference 5. The flow properties at the edge of the boundary layer were calculated by the computer program in reference 21.

Table I presents the results of the grit-on tests in the form of R_k (ref. 4). References 8 and 21 are used to obtain table I, also. In general, the roughness Reynolds numbers are greater than the critical values as given in figure 8 of reference 4. The present data are consistent with reference 4, since the transition location was moved forward by the presence of the roughness in all cases.

Sublimation Test Results

Interpretation of sublimation data requires an understanding of the technique and materials used to obtain the data. Higher skin friction causes the fluorene to sublimate faster. Due to the nature of the chemical and the skin-friction variation along the model, a pattern of coated area is formed by which the location of the transition region can be determined.

An equation which describes the time for the paint to sublimate may be derived from equations (15) and (43) in reference 22. The resulting expression is:

$$t = \frac{2\rho_c T_{surf} R_u h}{c_f p_v M_c u_\delta} \tag{1}$$

Since ρ_c, p_v, and M_c are functions of the chemical used and therefore are constant, and R_u is a constant and T_{surf} varies only slightly, these terms may be grouped into a constant. Thus,

$$t = K_1 \frac{h}{c_f u_\delta} \tag{2}$$

where

$$K_1 = \frac{2\rho_c T_{surf}}{p_v M_c} = \text{Constant}$$

The initial coating must be uniform over the model surface. If h varies along the model, the resulting pattern of painted regions will be meaningless. Thus, if h is constant:

$$t = K_2 \frac{1}{c_f u_\delta} \tag{3}$$

or

$$c_f = \frac{K_2}{t u_\delta} \tag{4}$$

where

$$K_2 = K_1 h$$

That is, the time required for the chemical to sublimate is inversely proportional to the skin-friction coefficient and the velocity just outside the boundary layer. The larger the skin friction and/or velocity, the shorter the time required for the paint to sublimate. If the velocity were constant along the model, the result would be

$$c_f = \frac{K_3}{t} \tag{5}$$

where

$$K_3 = \frac{K_2}{u_\delta}$$

In other words, the paint would sublimate fastest where the skin friction is highest. This result can be visualized by using a plot of skin friction along the model as in figure 9. At some time $t = t_0$, a line such as the dashed line in this figure may be visualized. The portions of this line lying below the longitudinal skin-friction-distribution curve are considered to be sublimated. That is, the dashed line represents values of K_3/t_0. Whenever this value is equal to the skin friction at a station, the fluorene is considered to be "wiped off" or sublimated and that area is left unpainted. (See eq. (5).) At some later time $t = t_1$, K_3/t_1 is obtained. The results in this figure show that at $t = t_2$ more paint has sublimated from the nose and a small region between point a and point b has also sublimated. The imaginary dashed line moves progressively downward with time until the model is entirely free of paint. At point c, photographs would show that the sublimation rate along the model decreases here, where dc_f/dx is relatively large.

This discussion has assumed that u_δ is constant along the body. Actually, u_δ varies slightly as shown in figure 10 because of the pressure gradient along the model. As a result of the variation of u_δ, the imaginary dashed curve is not actually horizontal or linear, as is shown in figure 11. The discussion of figure 9 applies to figure 11 also. Notice, however, that because of the slope in the K_2/tu_δ curves (eq. (4)), the chemical paint will sublimate off at the rear of the model before it sublimates near the transition region. The visualization in figure 11 shows sublimation will still occur at the nose first. As time progresses, the fluorene will sublimate from each end of the model toward the transition region. As in figure 9, when the fluorene sublimation rate along the model from the rear becomes a minimum (dx/dt is closest to zero) the painted-sublimated border should be near point c in figure 11. Thus, if the forward progression of the sublimated area is plotted as a function of time, the point where the slope is least will yield a position in the transition region. This is the procedure used in this study.

It should be noted that some sublimation investigations performed on flat plates and complete aircraft models (for example, ref. 23) appear to give clearer results than the ones presented in this report. The usual aircraft configuration tested uses roughness strips to induce transition farther upstream. These strips also cause the transition region to be more distinct and defined as shown in the pressure summary plots (fig. 6). Another important factor is that flat plates and aircraft model wings are easier to paint than a body of revolution. It is very difficult to apply an even thickness of paint to a body of revolution. Efforts were made to achieve a constant coating thickness h; however, it appears from some of the photographs that this effort was not completely

successful. Nevertheless, since the models were painted with a longitudinal "stroke" of the spray, the thickness along individual axial surface lines is relatively constant. The contour of the body of revolution also causes difficulty in the application of paint with constant thickness. Another factor contributing to the indistinctness of the transition region is the length of the transition region, particularly at the higher Mach numbers. The types of chemical used in sublimation tests vary widely. Different chemicals are needed for various tunnel test conditions. Chemicals are also available which require longer or shorter times for sublimation. Tables and charts to help the experimenter to select the chemical paint which best suits his test and tunnel are available (ref. 24, for example). The chemical used for this study was fluorene. The table in the instrumentation section gives some of the characteristics of fluorene.

In some cases the sublimation areas can readily be interpreted from the photographs themselves. However, because of the factors mentioned previously, it becomes necessary to plot the data as explained to obtain meaningful results. In plotting these data, a standard method must be used to measure the progression of the sublimated area toward the transition region. The point chosen for plotting is the most rearward point on the painted area. This choice is made for two reasons. First, since a specific axial "line" must be chosen to afford the most constant thickness and second, since the thicker paint coating (within reasonable limits) provides the clearest display of transition, the most rearward painted point should be on the thickest line and provide the best results.

Figure 12 illustrates the actual sequence of photographs from which the plots in figure 13 were derived. Figure 13 presents the distance from the model nose to the border between the painted and sublimated area as a function of time. The time is measured from an arbitrary initial time after the tunnel is operating at the desired flow conditions. The dashed line represents the point chosen as the transition location in accordance with the previous discussion.

Comparison of Sublimation and Impact-Pressure Results

The comparison of sublimation data and pressure data is shown in figure 14. This figure is arranged so that exact correspondence is indicated by the dashed line. For a given sublimation transition location there are two pressure transition locations indicated connected by a solid line. The left and right symbols represent the beginning and end of transition respectively from the impact pressure tests.

It was found that the sublimation technique tends to be less reliable than the impact pressure method mainly because of the difficulty of obtaining a constant chemical coating thickness over the model and uncertainty in the interpretation of the exact transition location from the sequence of photographs. The sublimation test gives only the transition location, whereas the impact-pressure-method results yield useful pressure information

over the model. However, sublimation tests are simple and very useful in determining approximate transition locations over complex structures such as entire aircraft configurations.

Force-Balance-Test Results

The data obtained in the force-balance test were reduced to the form of the drag coefficient, $C_{D,0}$. In figure 15, the drag coefficient is plotted against free-stream Reynolds number for each model with and without the roughness strip installed. The point at which the grit-on and grit-off curves become parallel approximately marks the beginning of almost fully turbulent flow on the model with grit off and the vertical distance between the two parallel curves indicated the drag caused by the roughness strip itself.

The roughness strip successfully induces turbulence near the nose of the model with only a slight amount of trip drag as shown in figure 15. For the lower Mach numbers, this drag caused by the roughness strip is less than 8 percent of the total drag of the model. At the higher Mach numbers, the Reynolds numbers tested do not extend high enough to show the beginning of natural fully turbulent flow and, therefore, the exact grit drag cannot be determined from these data. It should be noted that the Haack-Adams bodies of revolution tested are low-drag configurations and therefore 8 percent of the total model drag is a small amount compared with the drag normally occurring on fuselage and aircraft model configurations

Also shown in figure 15 are points which have been corrected for laminar-turbulent and fully turbulent flow from a skin-friction computer program for wind-tunnel models. Model shape, reference area, transition location, stagnation temperature, and free-stream Mach number and Reynolds number were input to the program. The transition location $x_{tr,b}$ was assumed to be at the local minimum of the impact pressure curve.

The computer program calculates the body skin-friction coefficient for the fully turbulent boundary layer and the mixed flow (laminar and then turbulent) boundary layer. The mixed flow calculations assume that the boundary-layer flow is laminar to the transition point. At the transition point the laminar and turbulent momentum thicknesses are assumed equal. A virtual origin of turbulent flow is then calculated. A step transition and fully turbulent flow rearward of the transition point are also assumed.

The skin-friction drag is determined by strip integration of the friction coefficient over the model surface using the Chapman and Rubesin method for laminar flow and the Karman-Schoenherr technique with the Sommer and Short T' method for turbulent flow (refs. 25 and 26).

The difference in the calculated fully turbulent and calculated mixed flow friction drag coefficients (which are both output by the skin-friction program) was then found and

added to the experimental mixed-flow drag coefficient (clean model) in figure 15. Ideally, the sum should correspond to the fully turbulent drag coefficient less the drag due to the roughness strip.

The results look reasonable since for $M_\infty = 2.00$ the dashed line passes through the fully turbulent results predicted by the program and the experimental mixed-flow results. Because the transition location was used in the skin-friction program to obtain the fully turbulent drag coefficient less grit drag, this good agreement supports the transition data obtained and used in this study.

CONCLUSIONS

Based on the impact pressure, sublimation, and force tests performed on bodies of revolution at zero angle of attack with and without grit under a range of tests conditions considered in this study several conclusions may be made.

1. The carborundum roughness strip (average height 0.025 cm) near the model nose was found to induce nearly complete turbulent flow over the models at the lower Mach numbers and higher Reynolds number considered while increasing the overall drag by less than 8 percent of the drag of the model with transition fixed.

2. The grit-on data obtained are generally consistent with previous analytical data from NASA TN D-3579 and AEDC TR-60-5.

3. The plotting of the location of the sublimated-painted border against time in the sublimation test resulted in good agreement between the sublimation and impact pressure methods. However, the impact-pressure technique seemed more reliable on the type of model used in this study.

Langley Research Center,
National Aeronautics and Space Administration,
Hampton, Va., September 15, 1970.

REFERENCES

1. Smith, A. M. D.; and Clutter, Darwin W.: The Smallest Height of Roughness Capable of Affecting Boundary-Layer Transition. J. Aero/Space Sci., vol. 26, no. 4, Apr. 1959, pp. 229-245, 256.

2. Potter, J. Leith; and Whitfield, Jack D.: Effects of Slight Nose Bluntness and Roughness on Boundary-Layer Transition in Supersonic Flows. J. Fluid Mech., vol. 12, pt. 4, Apr. 1962, pp. 501-535.

3. Braslow, Albert L.: Review of the Effect of Distributed Surface Roughness on Boundary-Layer Transition. AGARD Rep. 254, Apr. 1960.

4. Braslow, Albert L.; Hicks, Raymond M.; and Harris, Roy V., Jr.: Use of Grit-Type Boundary-Layer-Transition Trips on Wind-Tunnel Models. NASA TN D-3579, 1966.

5. Potter, J. Leith; and Whitfield, Jack D.: Effects of Unit Reynolds Number, Nose Bluntness, and Roughness on Boundary Layer Transition. AEDC-TR-60-5, U.S. Air Force, Mar. 1960.

6. Sterrett, James R.; Morrisette, E. Leon; Whitehead, Allen H., Jr.; and Hicks, Raymond M.: Transition Fixing in Hypersonic Flow. NASA TN D-4129, 1967.

7. Czarnecki, K. R.; and Sinclair, Archibald R.: Factors Affecting Transition at Supersonic Speeds. NACA RM L53I18a, 1953.

8. Braslow, Albert L.; and Knox, Eugene C.: Simplified Method for Determination of Critical Height of Distributed Roughness Particles for Boundary-Layer Transition at Mach Numbers From 0 to 5. NACA TN 4363, 1958.

9. Von Doenhoff, Albert E.; and Braslow, Albert L.: The Effect of Distributed Surface Roughness on Laminar Flow. Boundary Layer and Flow Control, Vol. 2, G. V. Lachmann, ed., Pergamon Press, 1961.

10. Holloway, Paul F.; and Sterrett, James R.: Effect of Controlled Surface Roughness on Boundary-Layer Transition and Heat Transfer at Mach Numbers of 4.8 and 6.0. NASA TN D-2054, 1964.

11. Van Driest, E. R.; and McCauley, W. D.: Effect of Controlled Three-Dimensional Roughness on Boundary-Layer Transition at Supersonic Speeds. J. Aero/Space Sci., vol. 27, no. 4, Apr. 1960, pp. 261-271, 303.

12. Van Driest, E. R.; and Blumer, C. B.: Effect of Roughness on Transition in Supersonic Flow. AGARD Rep. 255, Apr. 1960.

13. Klebanoff, P. S.; Schubauer, G. B.; and Tidstrom, K. D.: Measurements of the Effect of Two-Dimensional and Three-Dimensional Roughness Elements on Boundary-Layer Transition. J. Aeronaut. Sci., vol. 22, no. 11, Nov. 1955, pp. 803-804.

14. Peterson, John B., Jr.: Boundary-Layer Velocity Profiles Downstream of Three-Dimensional Transition Trips on a Flat Plate at Mach 3 and 4. NASA TN D-5523, 1969.

15. Tani, Itiro; Hama, Francis R.; and Mituisi, Satosi: On the Effect of a Single Roughness Element on Boundary-Layer Transition. Rep. Inst. Sci. Technol., vol. 8, no. 3, Toyko Univ., May 1954, pp. 125-133.

16. Adams, Mac C.: Determination of Shapes of Boattail Bodies of Revolution for Minimum Wave Drag. NACA TN 2550, 1951.

17. Harris, Roy V., Jr.; and Landrum, Emma Jean: Drag Characteristics of a Series of Low-Drag Bodies of Revolution at Mach Numbers From 0.6 to 4.0. NASA TN D-3163, 1965.

18. Sax, N. Irving: Dangerous Properties of Industrial Materials. Second ed., Reinhold Pub. Corp., 1963.

19. Stecker, Paul G., ed.: The Merck Index. Eighth ed., Merck & Co., Inc., 1968.

20. Hodgman, Charles D.; Weast, Robert C.; and Selby, Samuel M.; eds.: Handbook of Chemistry and Physics. Forty-second ed., Chem. Rubber Pub. Co., c.1960.

21. Jackson, Charlie M., Jr.; and Smith, Rudeen S.: A Method for Determining the Total Drag of a Pointed Body of Revolution In Supersonic Flow With Turbulent Boundary Layer. NASA TN D-5046, 1969.

22. Owen, P. R.; and Ormerod, A. O.: Evaporation From the Surface of a Body in an Airstream With Particular Reference to the Chemical Method of Indicating Boundary-Layer Transition. R & M No. 2875, Brit. A.R.C., 1954.

23. Vaucheret, Xavier: Déclenchement Artificiel de la Transition en Supersonique. La Recherche Aérospatiale, no. 120, Sept.-Oct. 1967, pp. 25-32. (Available as NASA TT F-11,558.)

24. Main-Smith, J. D.: Chemical Solids as Diffusible Coating Films for Visual Indications of Boundary-Layer Transition in Air and Water. R & M No. 2755, British A.R.C., 1950.

25. Chapman, Dean R.; and Rubesin, Morris W.: Temperature and Velocity Profiles in the Compressible Laminar Boundary Layer With Arbitrary Distribution of Surface Temperature. J. Aeronaut. Sci., vol. 16, no. 9, Sept. 1949, pp. 547-565.

26. Sommer, Simon C.; and Short, Barbara J.: Free-Flight Measurements of Turbulent-Boundary-Layer Skin Friction in the Presence of Severe Aerodynamic Heating at Mach Numbers From 2.8 to 7.0. NACA TN 3391, 1955.

TABLE I.- RESULTS OF GRIT-ON TESTS

M_∞	$R_{l,\infty}$	M_δ	$R_{x,k}$	R_k	k/δ
			Model A		
2.00	6×10^6	1.85	0.268×10^6	2179	0.96
	9	1.85	.326	2650	1.03
	12	1.85	.434	3528	1.13
2.75	6	2.51	.229	1651	.80
	9	2.51	.342	3070	.98
	15	2.51	.572	4650	1.11
4.63	6	3.96	.253	252	.56
	9	3.96	.381	1753	.69
	12	3.96	.510	2428	.80
	15	3.96	.633	3978	.89
			Model B		
2.00	3×10^6	1.78	0.111×10^6	666	0.64
	6	1.78	.226	1997	.95
	9	1.78	.339	2701	1.04
2.75	6	2.39	.238	1781	.85
	9	2.39	.357	2845	.96
	15	2.39	.602	4797	1.405
4.63	6	3.66	.247	373	.61
	9	3.66	.370	1216	.75
	12	3.66	.493	2949	.86
	15	3.66	.614	4937	.98
			Model C		
2.75	6×10^6	2.14	0.249×10^6	1871	0.87
	9	2.14	.373	2847	1.00
	15	2.14	.622	4748	1.18
4.63	9	3.09	.341	1869	.80
	12	3.09	.453	3533	.92
	15	3.09	.563	4298	1.03

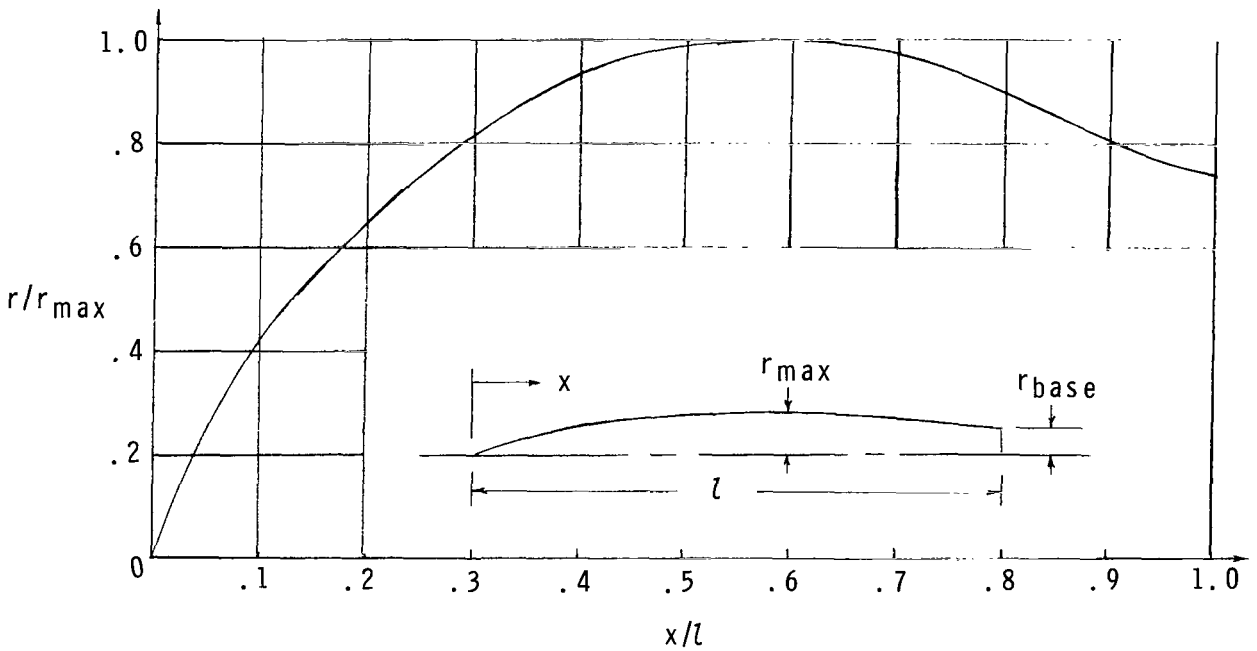

Figure 1.- Longitudinal distribution of body radii for Haack-Adams bodies of revolution.

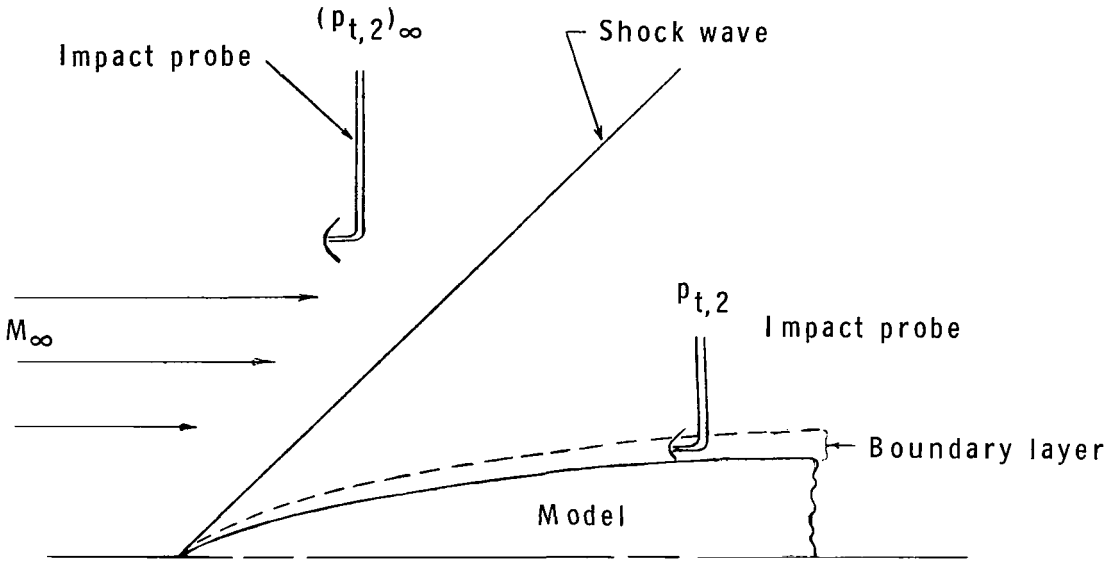

(a) Schematic of probe placement.

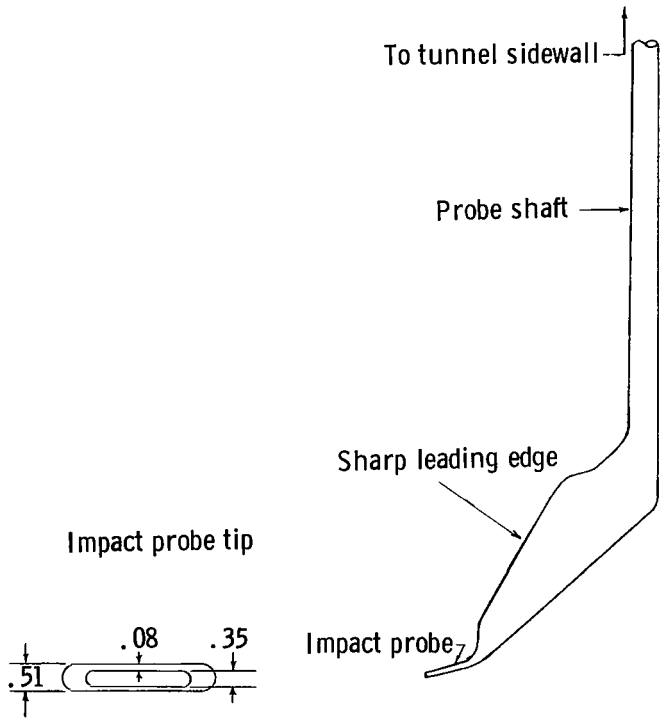

(b) Sketch of probe.

Figure 2.- Impact probe sketches.

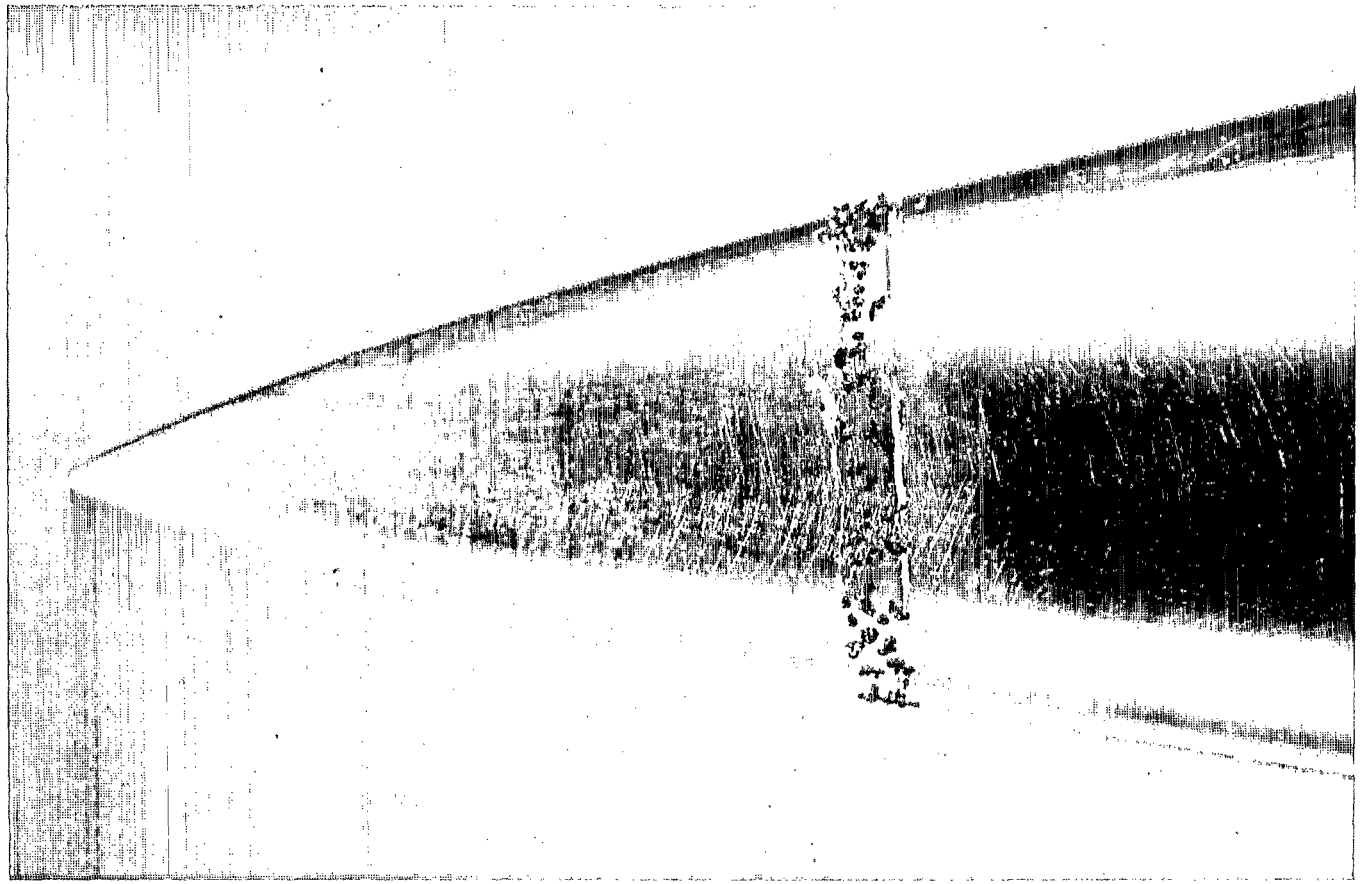

L-70-2710

Figure 3.- Photograph of roughness strip.

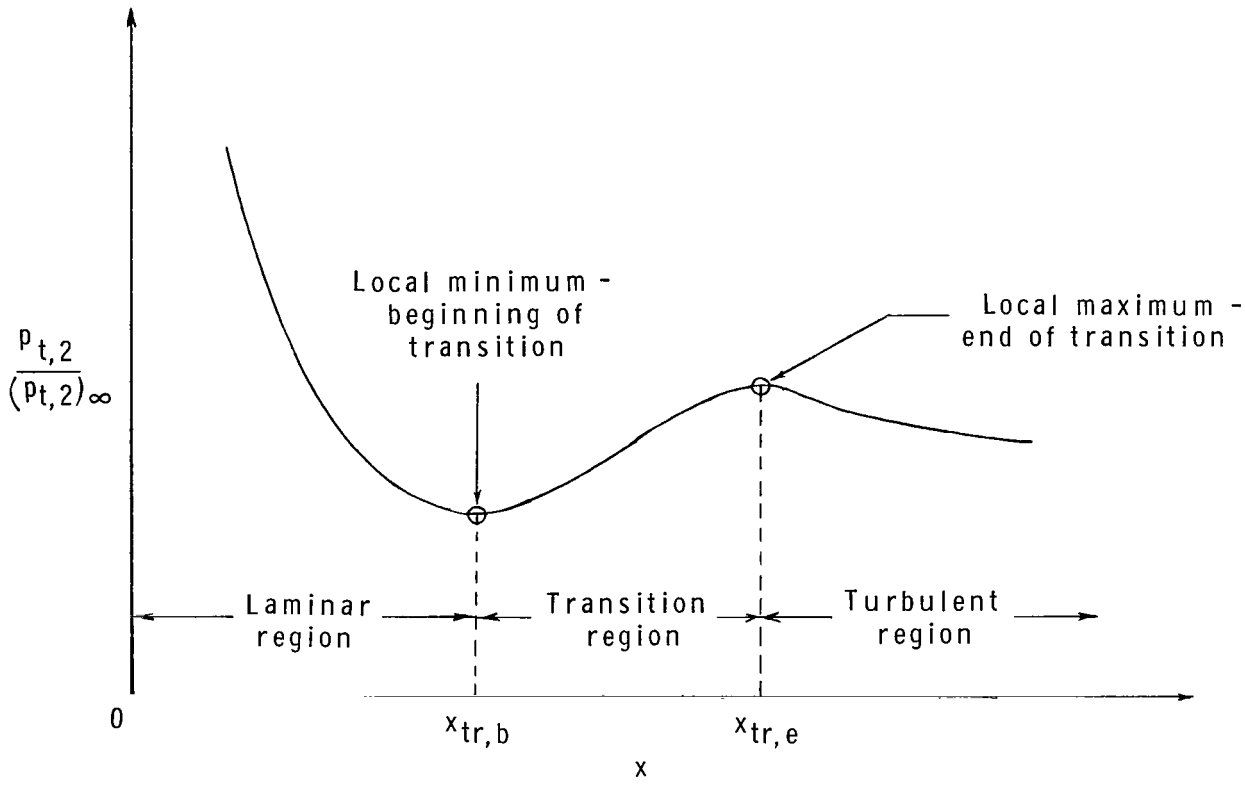

Figure 4.- The transition region.

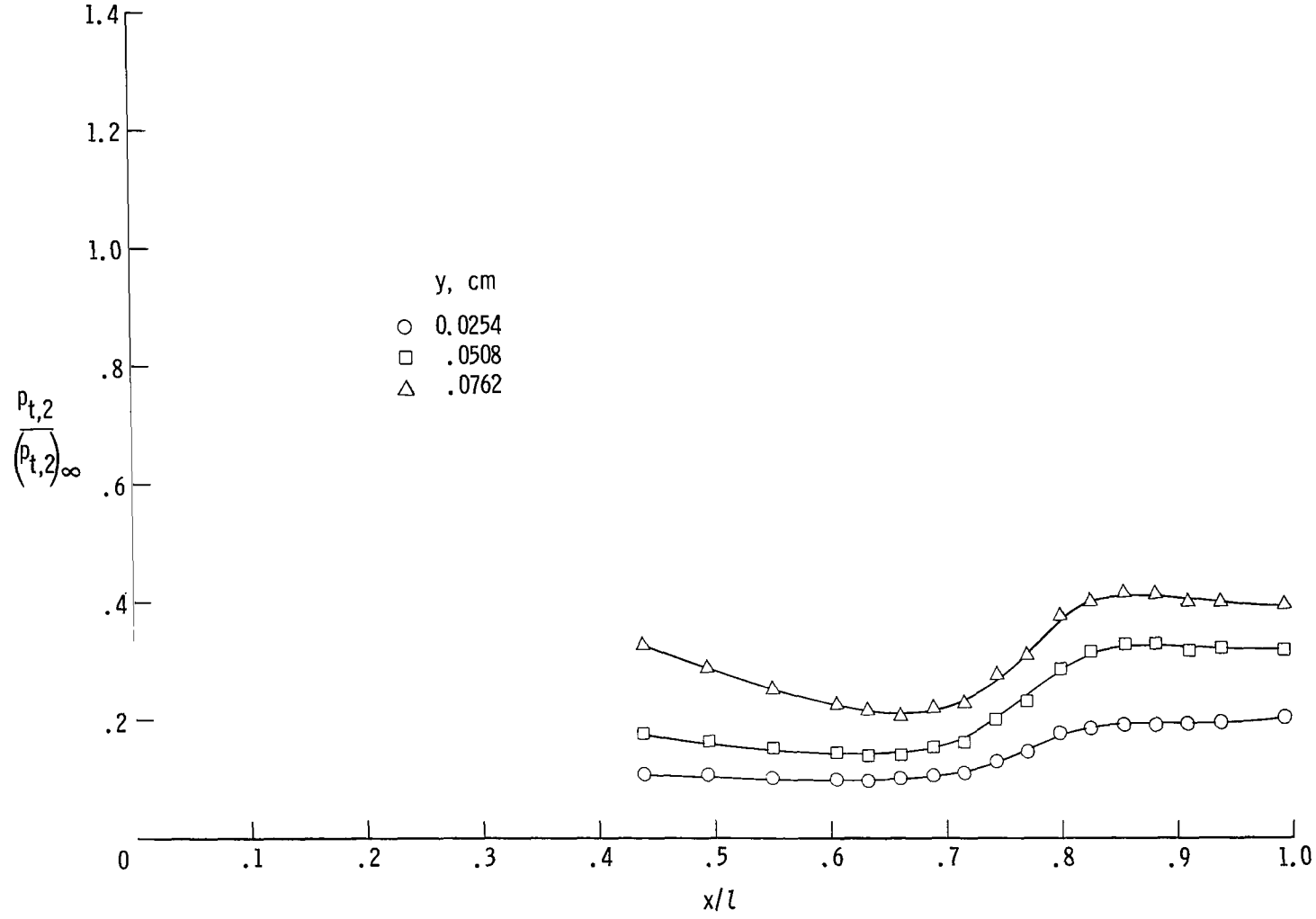

(a) Model A, grit off; $M_\infty = 2.75$; $R_{l,\infty} = 6 \times 10^6$.

Figure 5.- Longitudinal impact-pressure distribution.

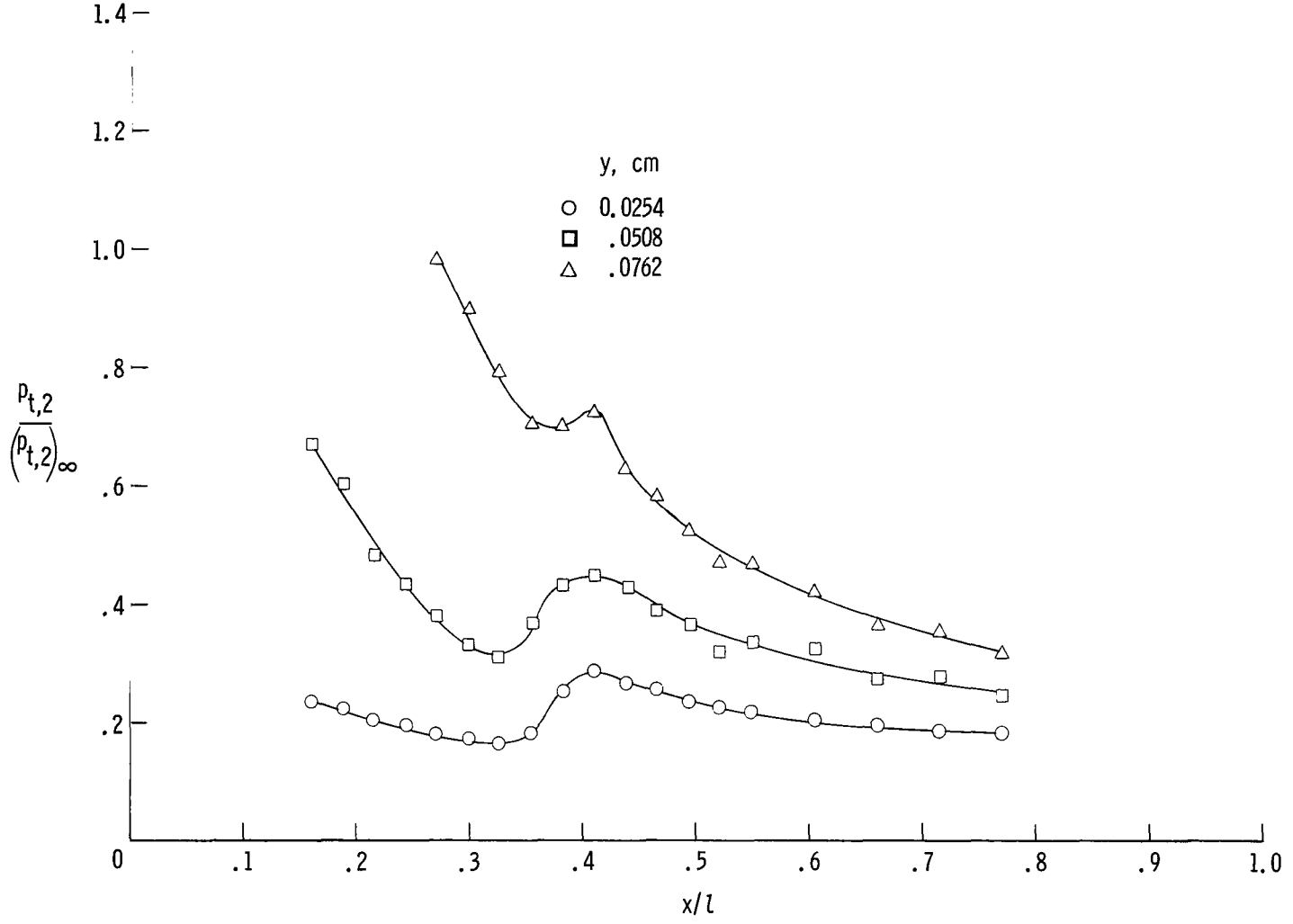

(b) Model A, grit off; $M_\infty = 2.75$, $R_{l,\infty} \approx 15 \times 10^6$.

Figure 5.- Continued.

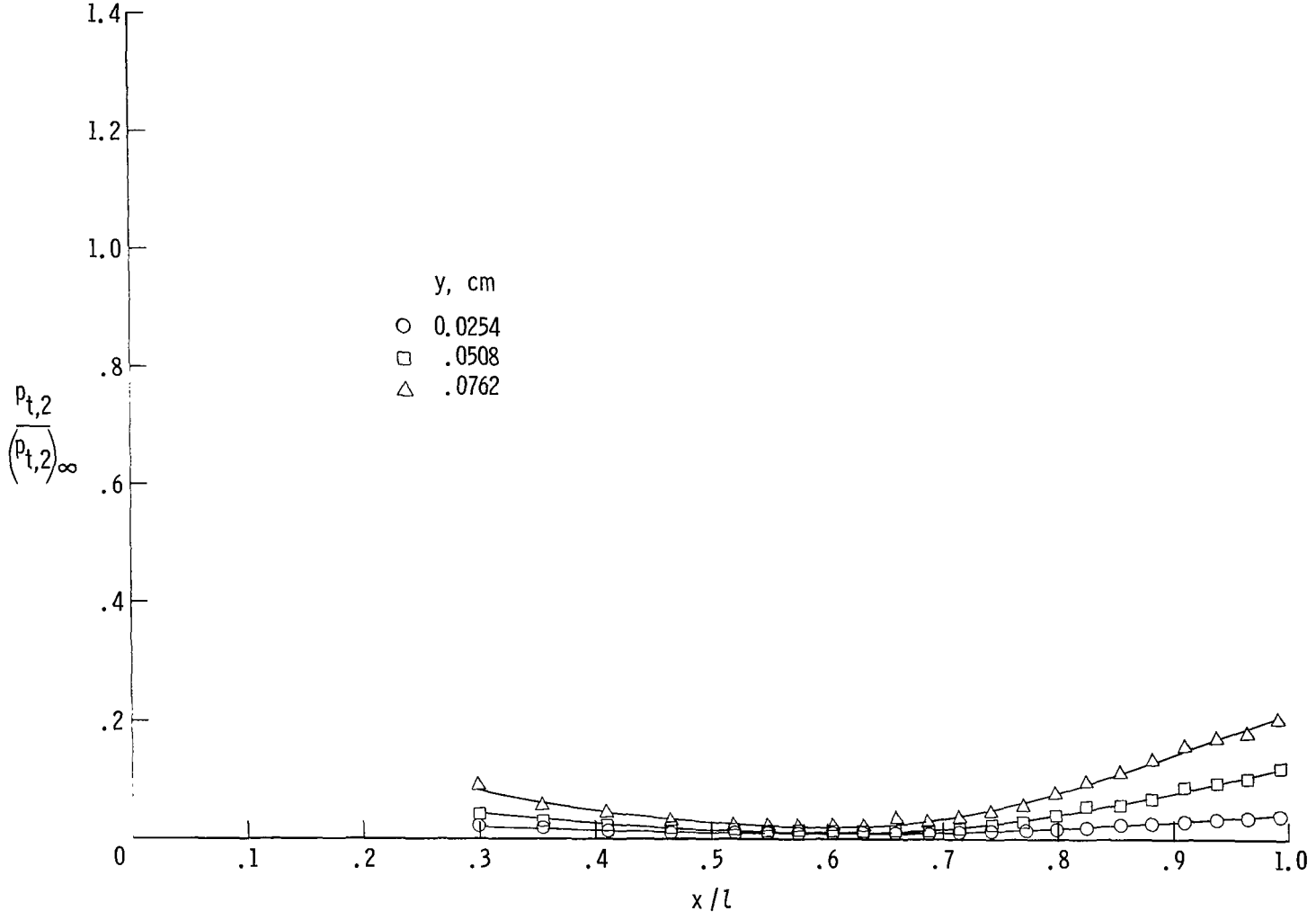

(c) Model A, grit off; $M_\infty = 4.63$; $R_{l,\infty} \approx 6 \times 10^6$.

Figure 5.- Continued.

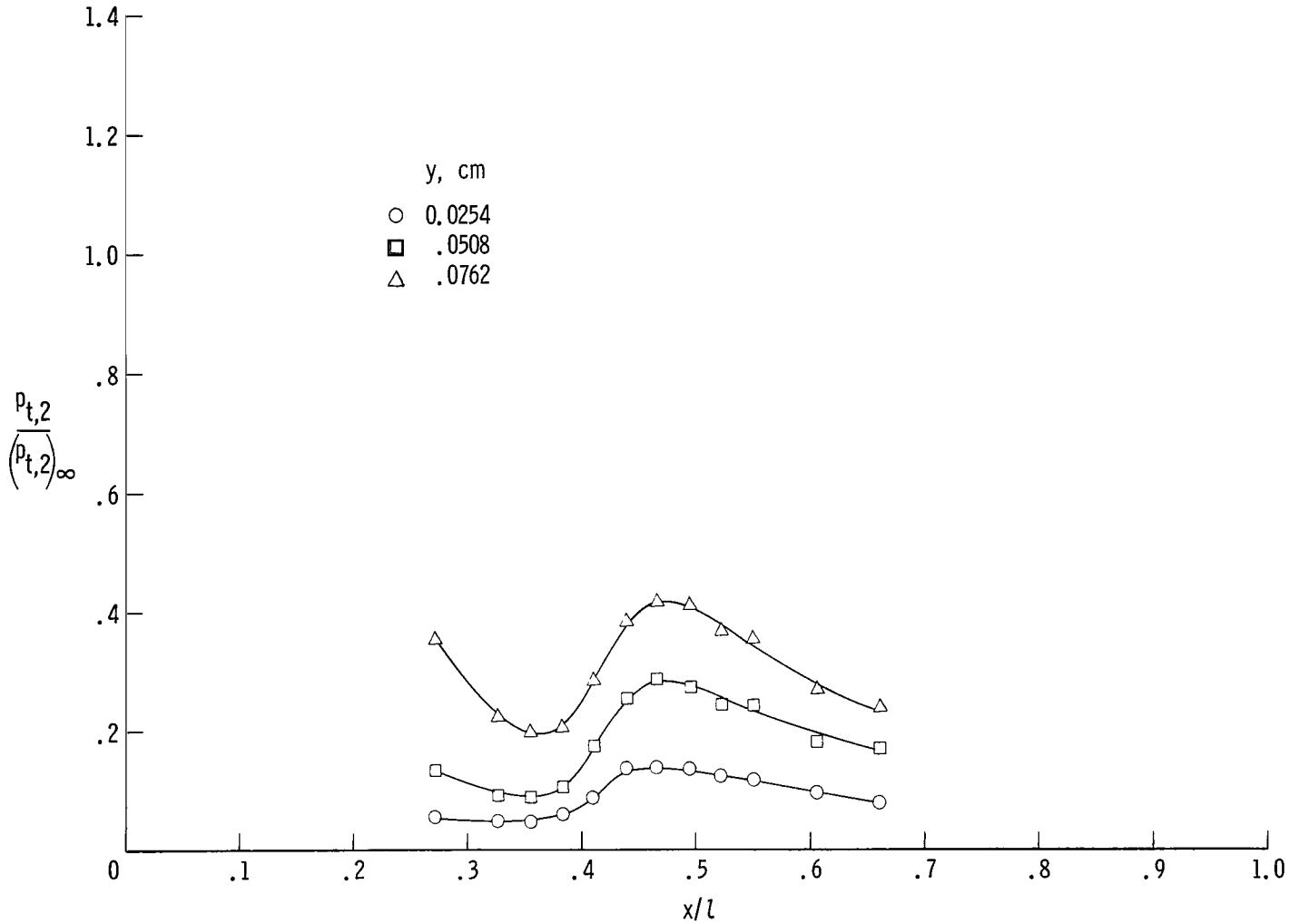

(d) Model A, grit off; $M_\infty = 4.63$; $R_{l,\infty} \approx 15 \times 10^6$.

Figure 5.- Continued.

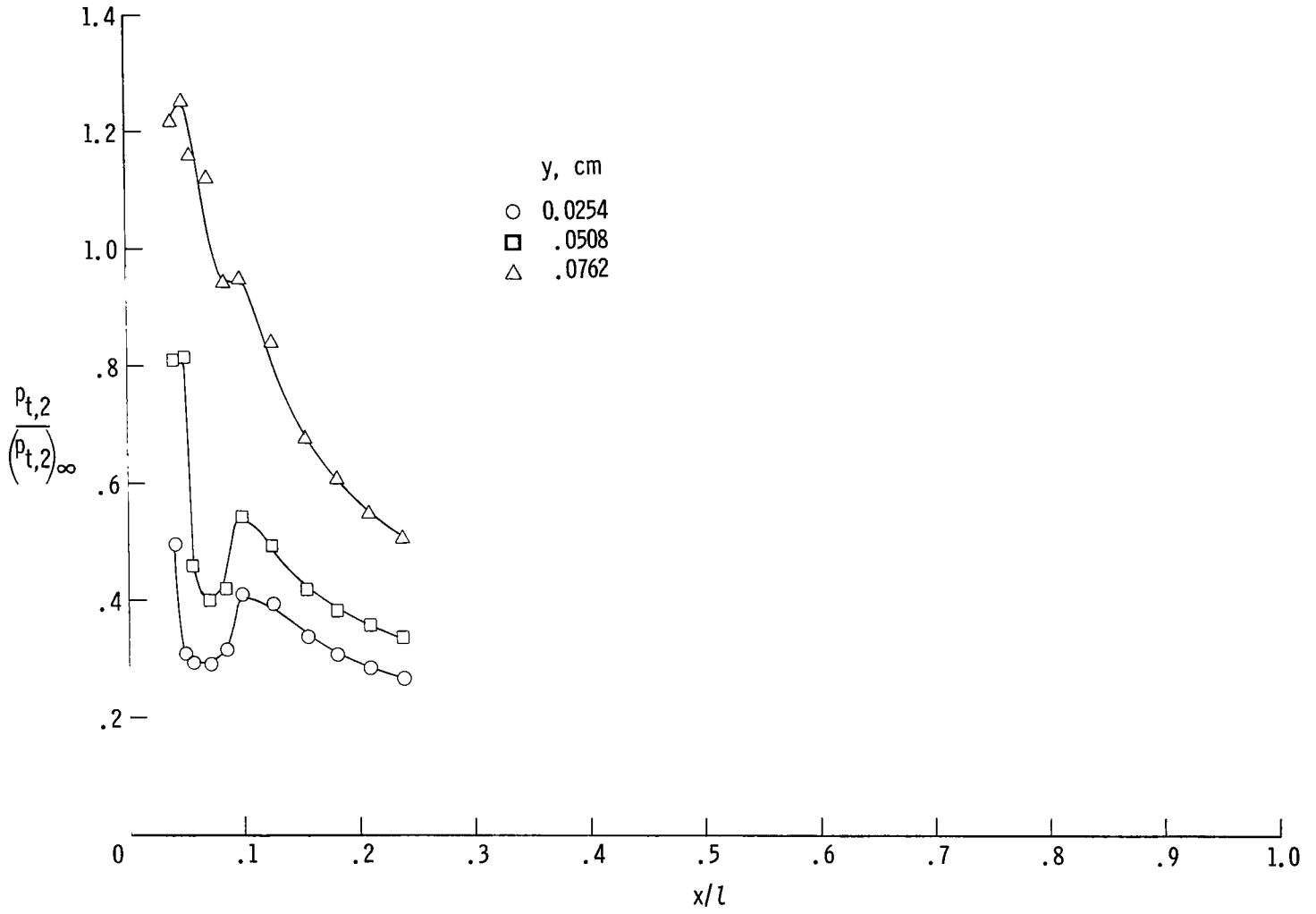

(e) Model A, grit on; $M_\infty = 2.75$; $R_{l,\infty} \approx 6 \times 10^6$.

Figure 5.- Continued.

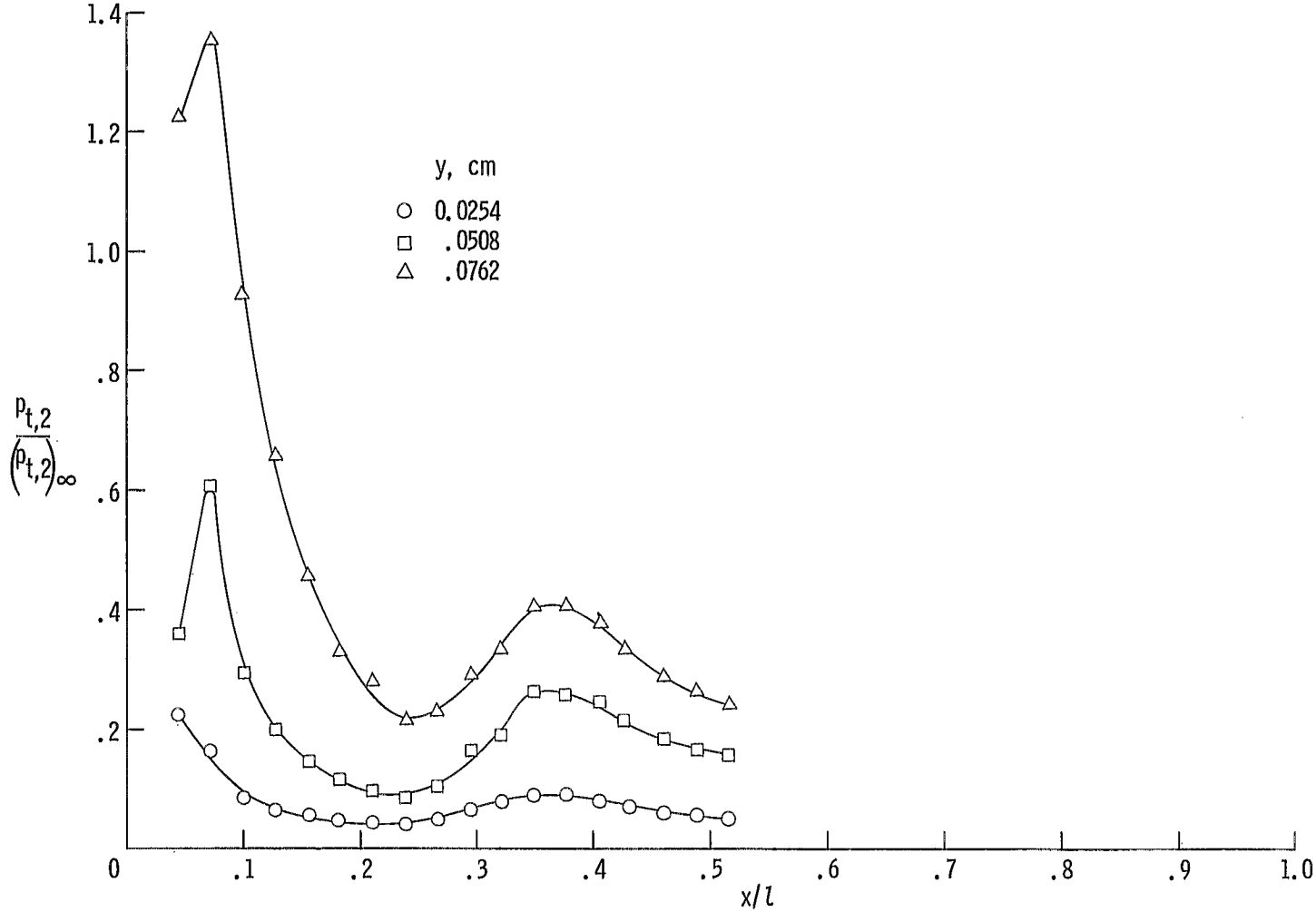

(f) Model A, grit on; $M_\infty = 4.63$; $R_{l,\infty} \approx 9 \times 10^6$.

Figure 5.- Continued.

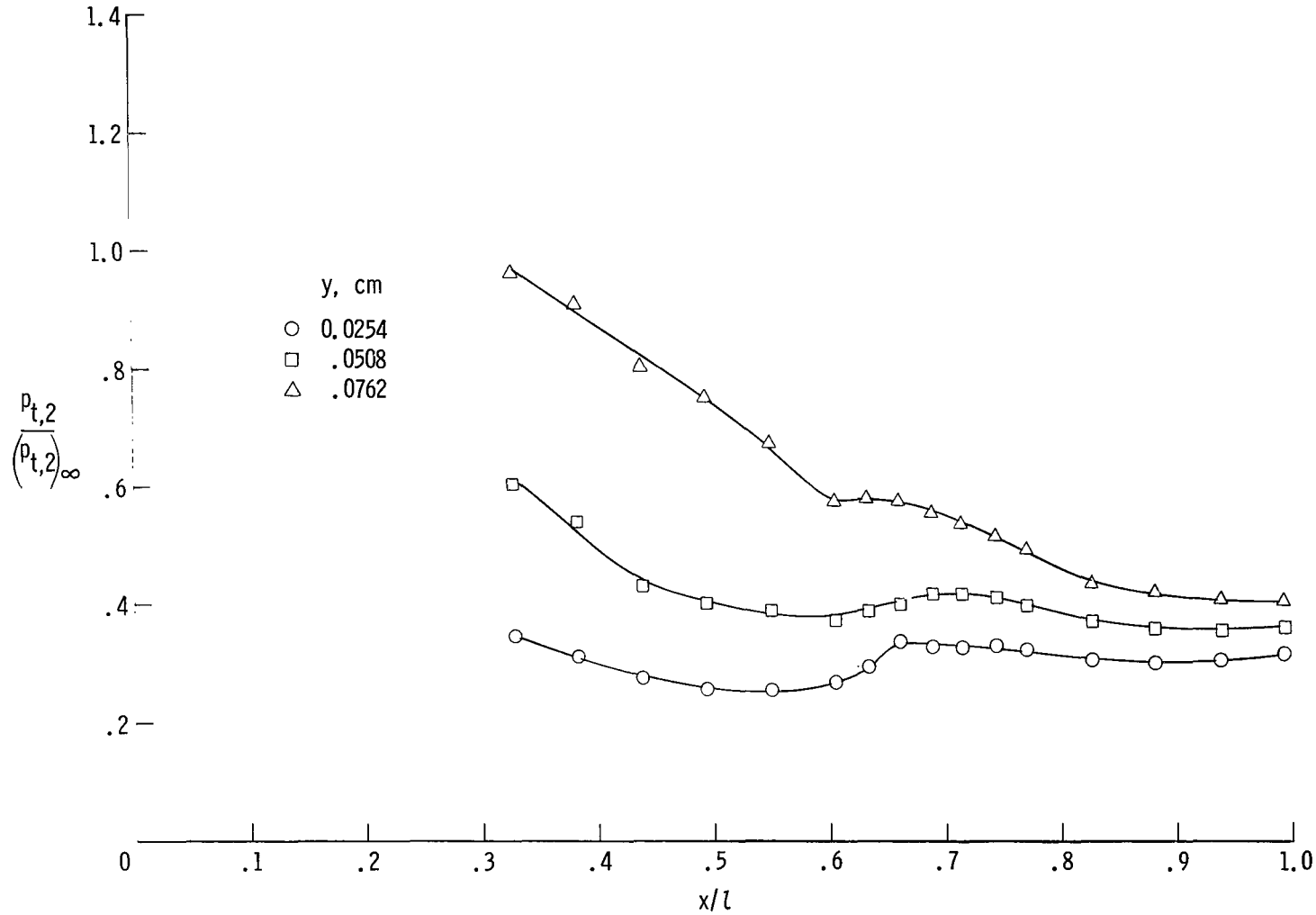

(g) Model B, grit off; $M_\infty = 2.00$; $R_{l,\infty} \approx 9 \times 10^6$.

Figure 5.- Continued.

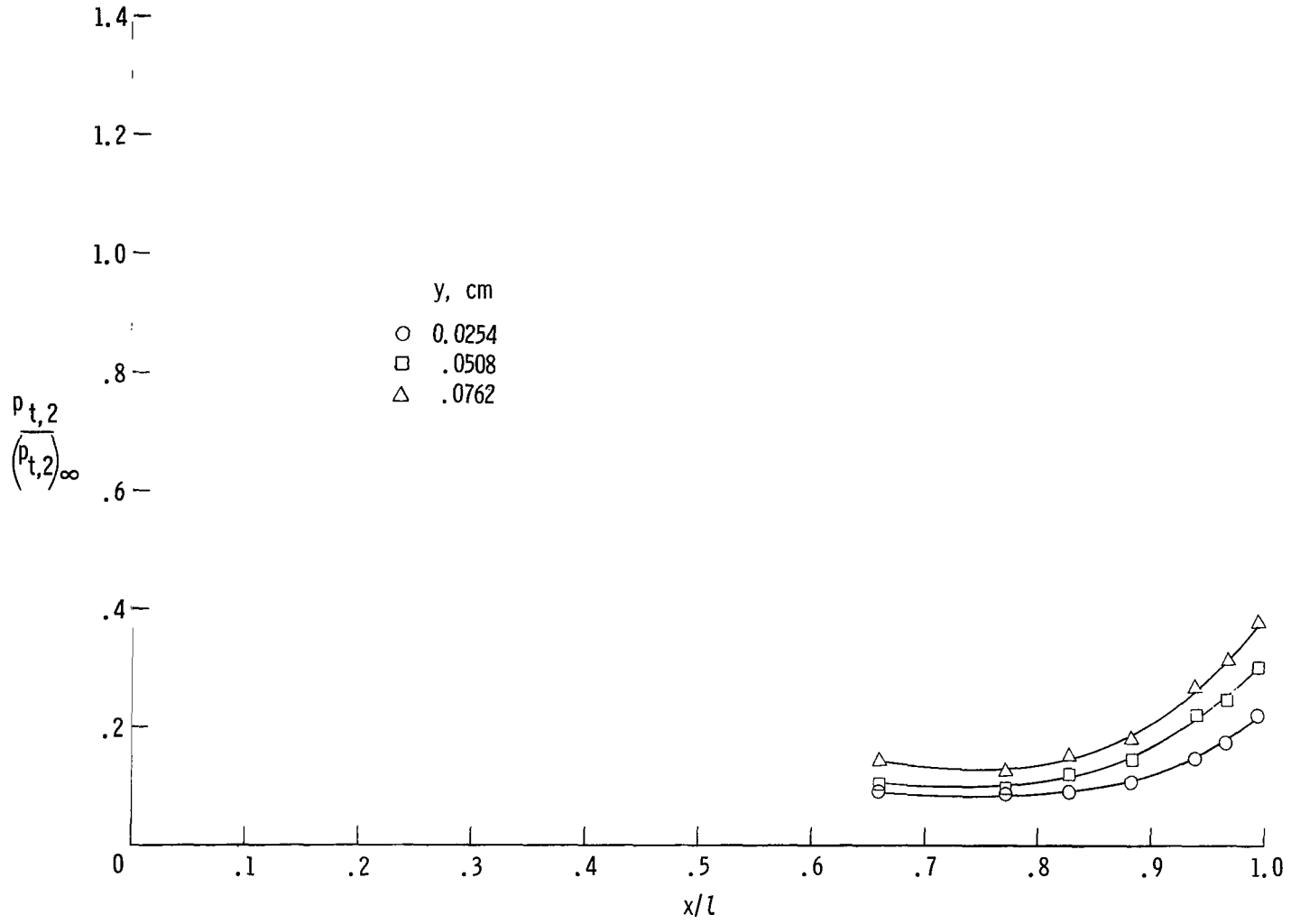

(h) Model B, grit off; $M_\infty = 2.75$; $R_{l,\infty} \approx 6 \times 10^6$.

Figure 5.- Continued.

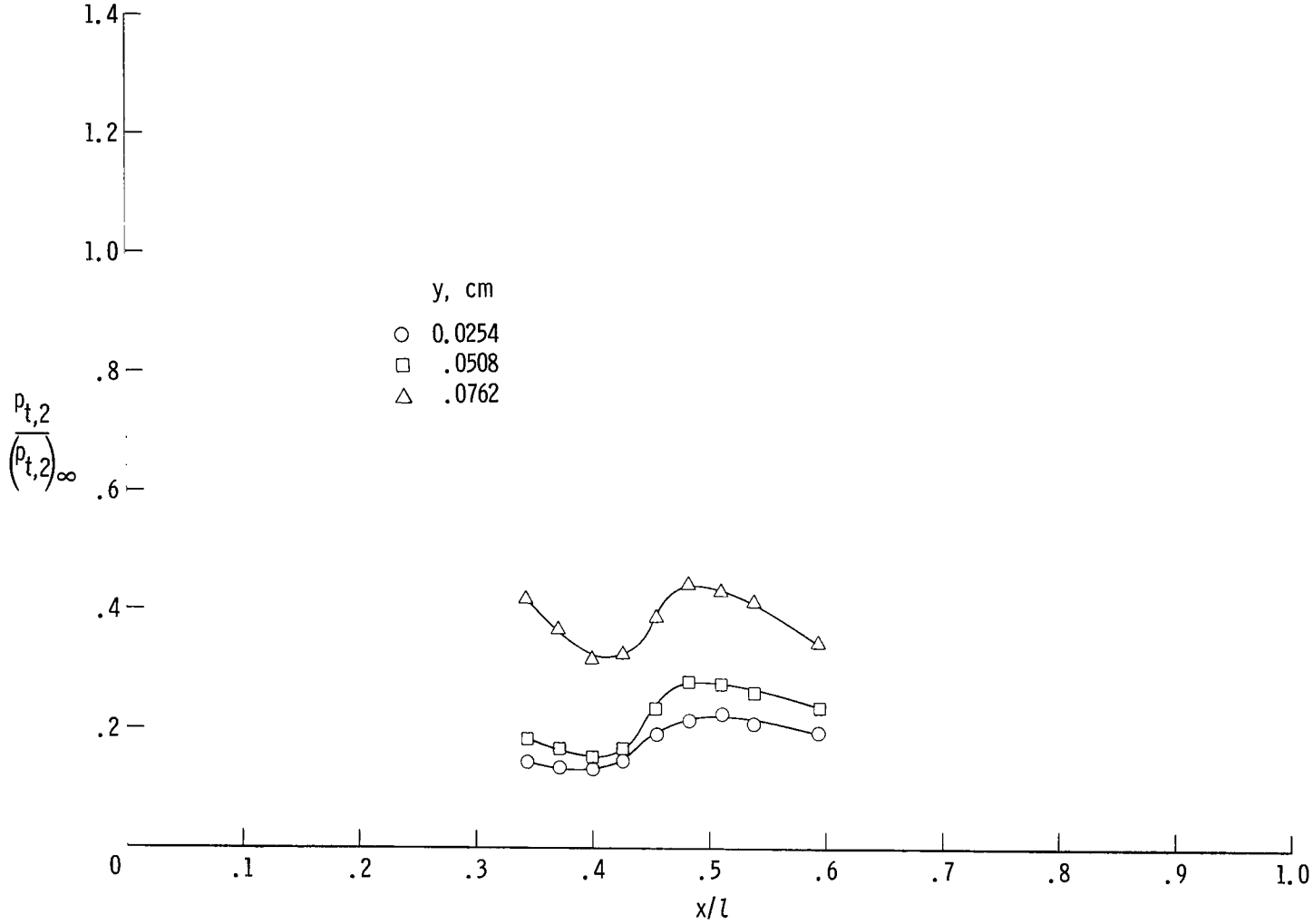

(i) Model B, grit off; $M_\infty = 2.75$; $R_{l,\infty} \approx 15 \times 10^6$.

Figure 5.- Continued.

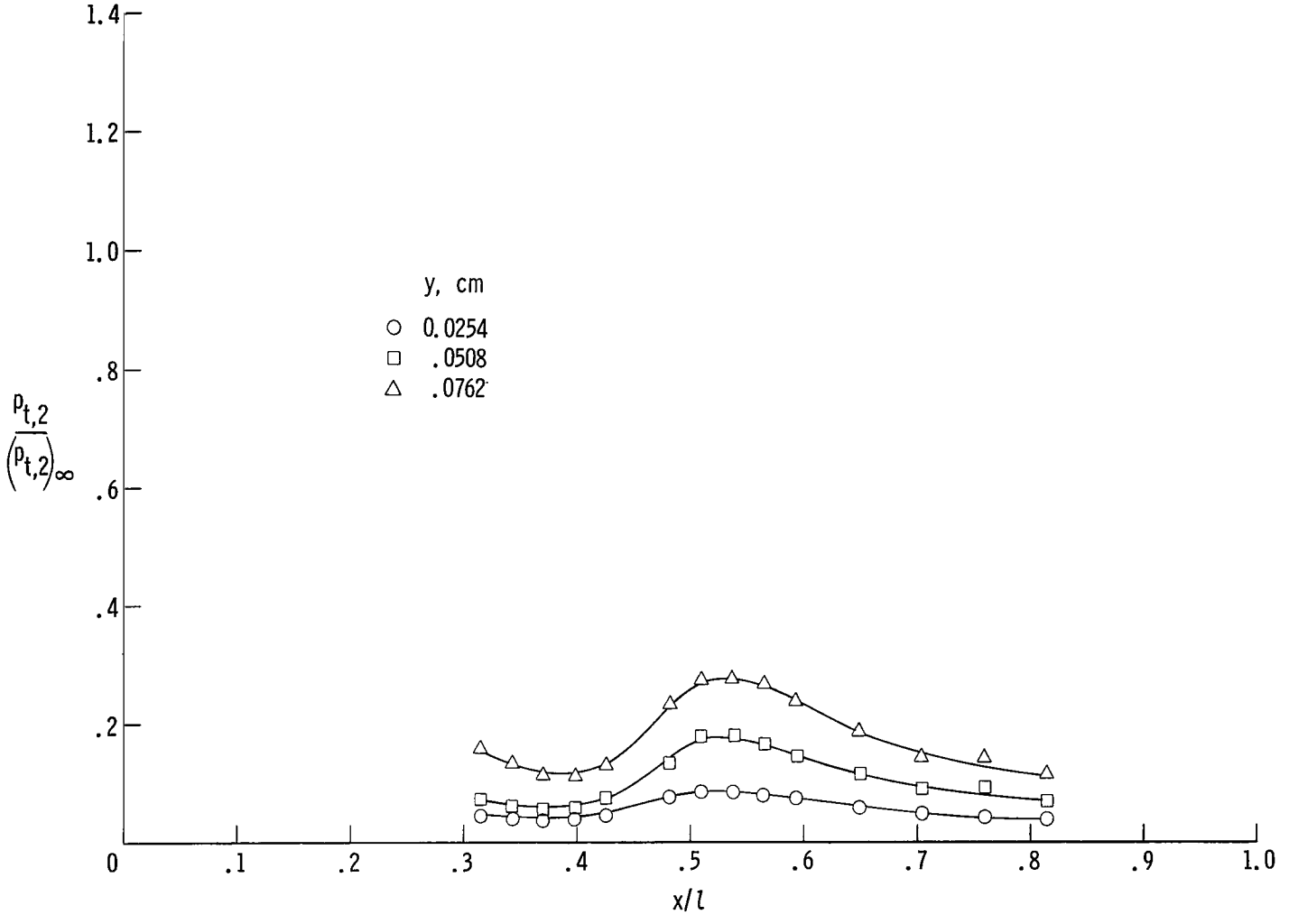

(j) Model B, grit off; $M_\infty = 4.63$; $R_{l,\infty} \approx 15 \times 10^6$.

Figure 5.- Continued.

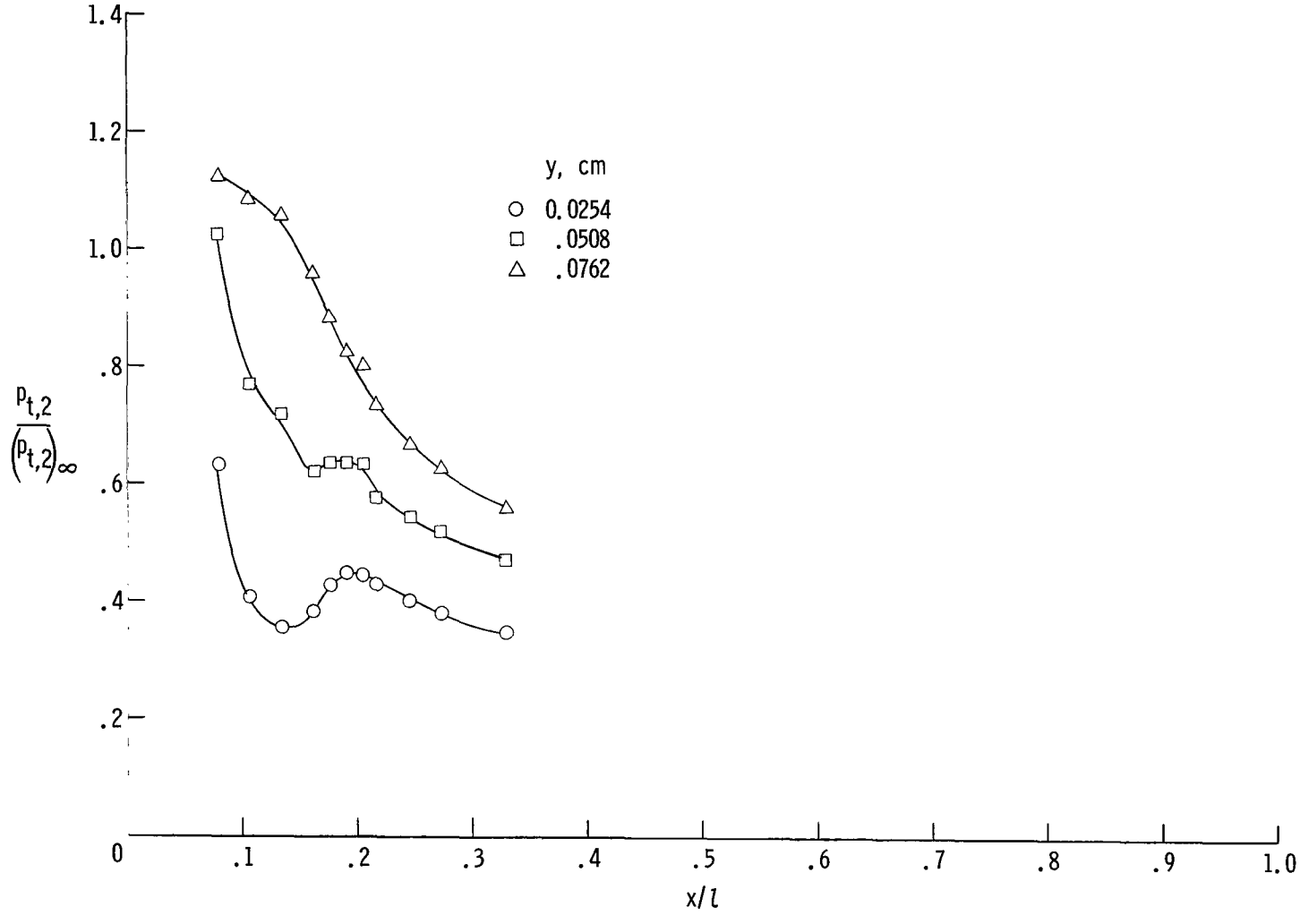

(k) Model B, grit on; $M_\infty = 2.00$; $R_{l,\infty} \approx 3 \times 10^6$.

Figure 5.- Continued.

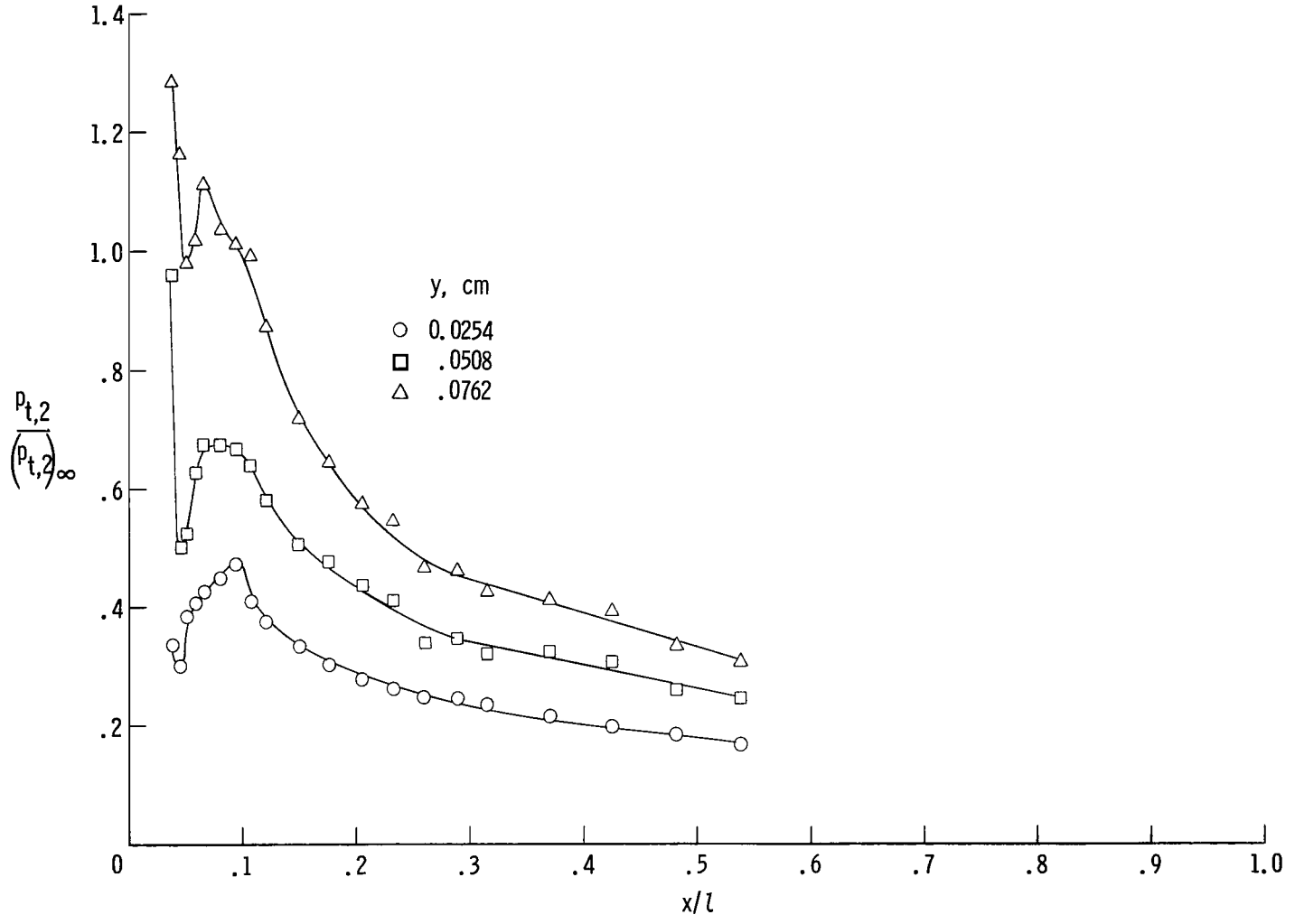

(l) Model B, grit on; $M_\infty = 2.75$; $R_{l,\infty} \approx 6 \times 10^6$.

Figure 5.- Continued.

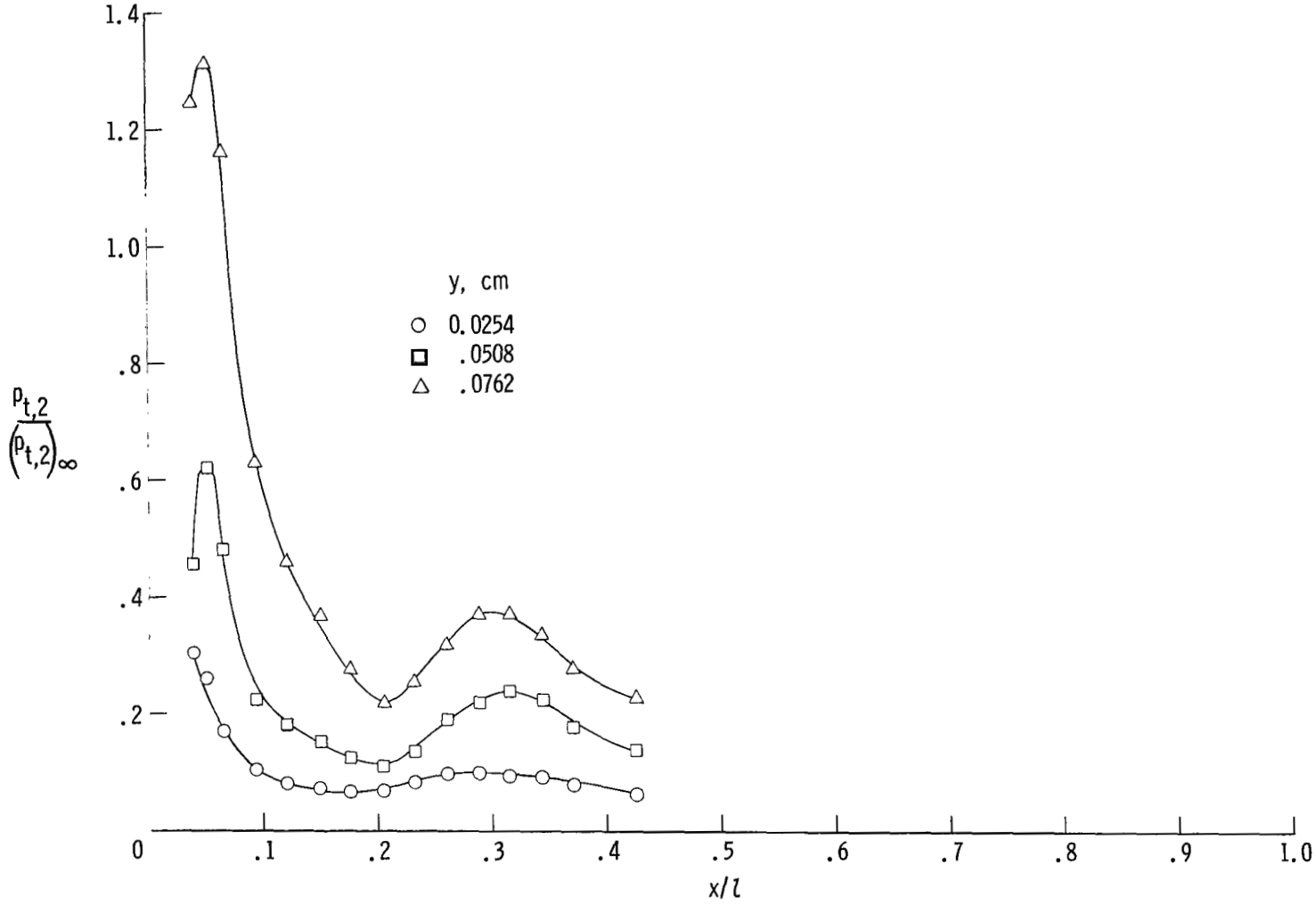

(m) Model B, grit on; $M_\infty = 4.63$; $R_{l,\infty} \approx 9 \times 10^6$.

Figure 5.- Continued.

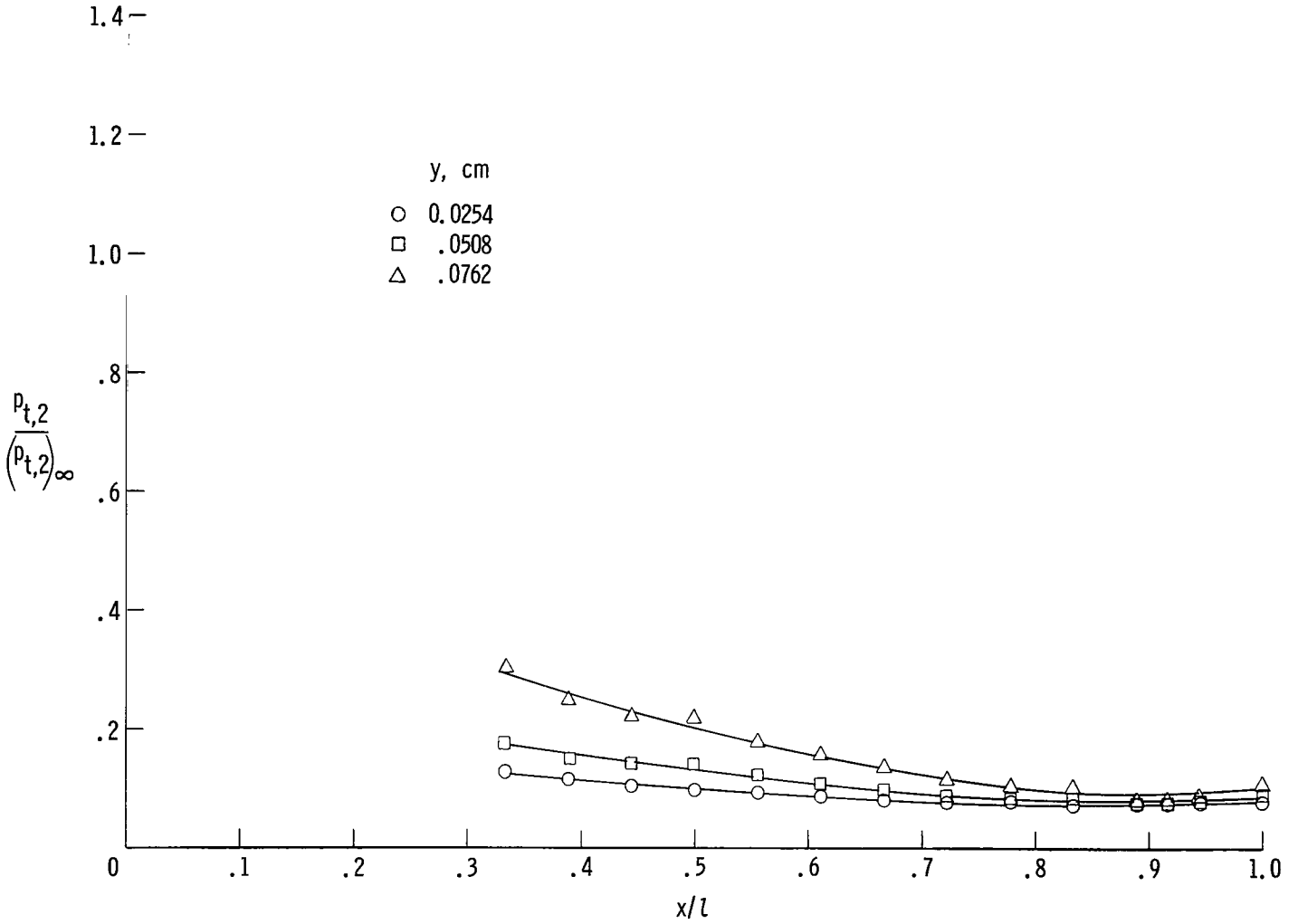

(n) Model C, grit off; $M_\infty = 2.75$, $R_{l,\infty} \approx 6 \times 10^6$.

Figure 5.- Continued.

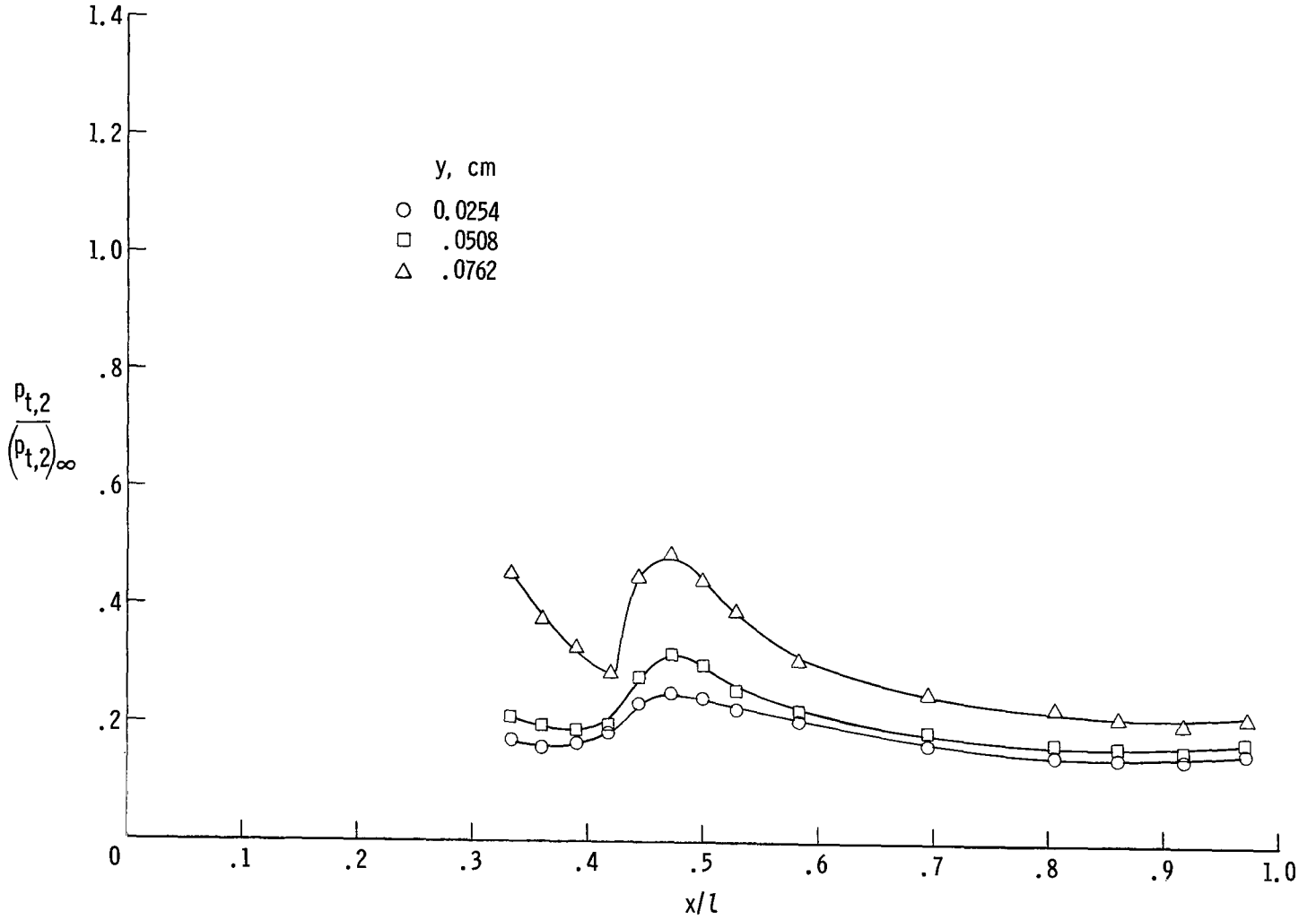

(o) Model C, grit off; $M_\infty = 2.75$; $R_{l,\infty} \approx 15 \times 10^6$.

Figure 5.- Continued.

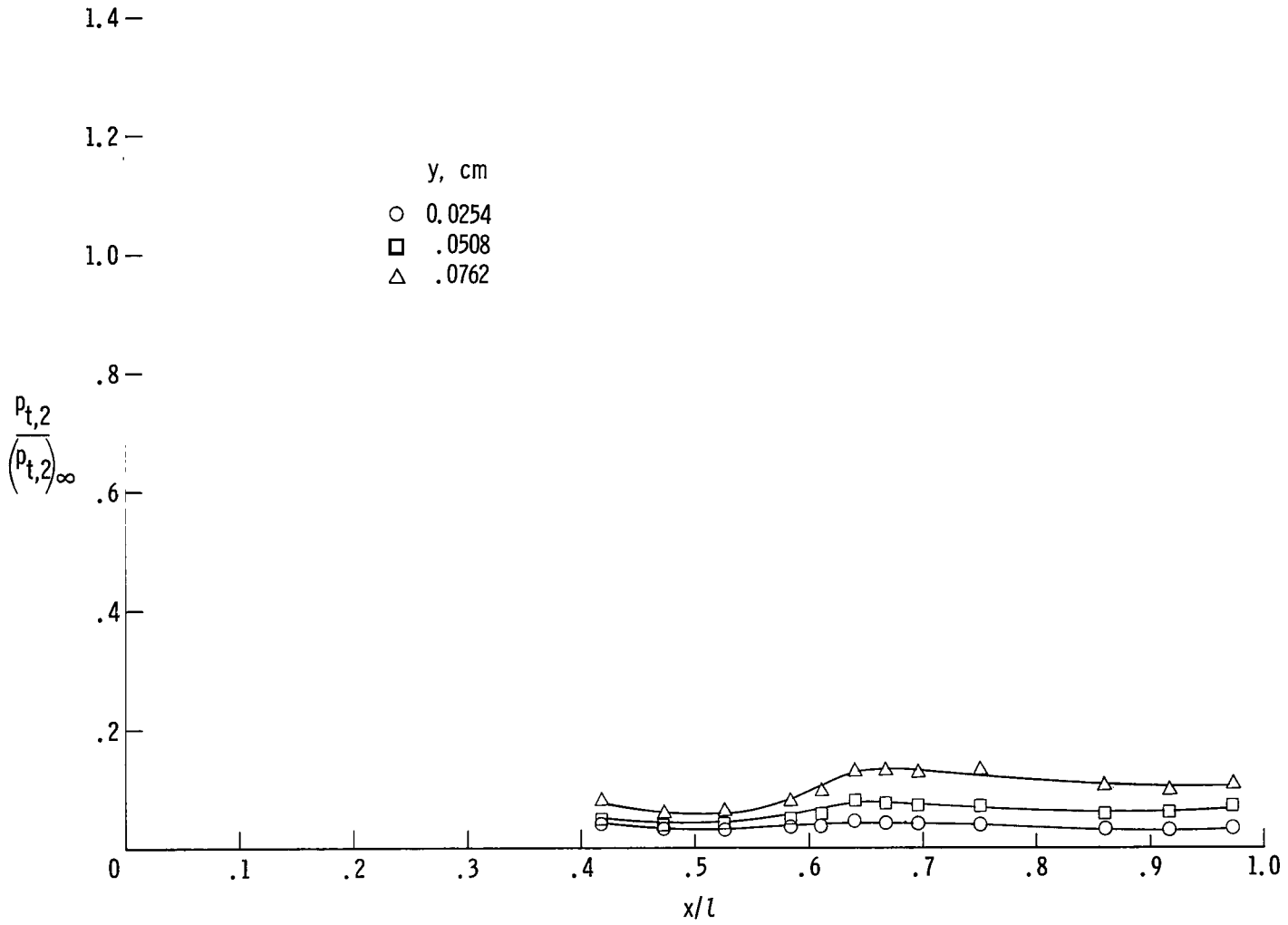

(p) Model C, grit off; $M_\infty = 4.63$; $R_{l,\infty} \approx 15 \times 10^6$.

Figure 5.- Continued.

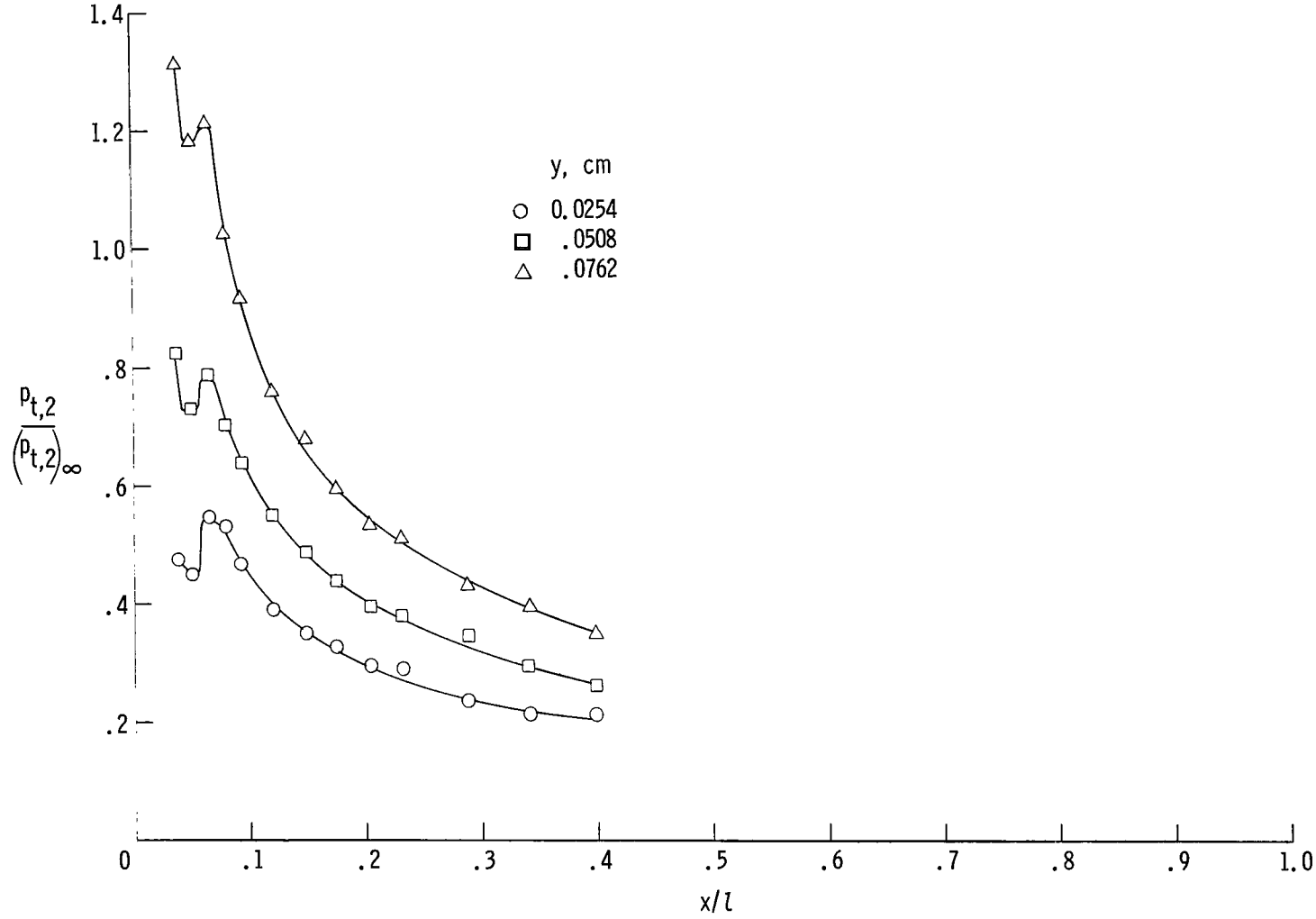

(q) Model C, grit on; $M_\infty = 2.75$; $R_{l,\infty} \approx 6 \times 10^6$.

Figure 5.- Continued.

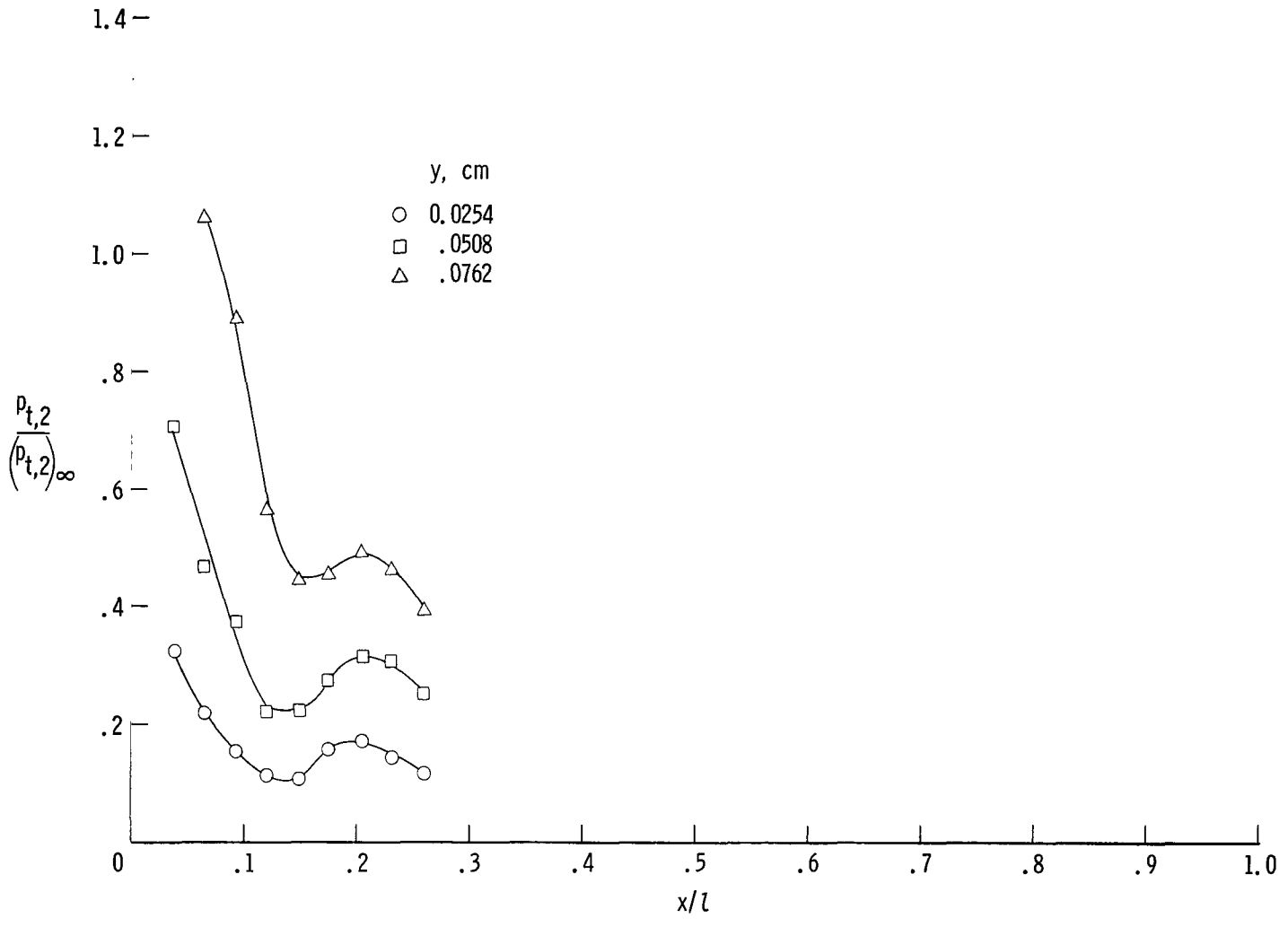

(r) Model C, grit on; $M_\infty = 4.63$; $R_{l,\infty} \approx 9 \times 10^6$.

Figure 5.- Concluded.

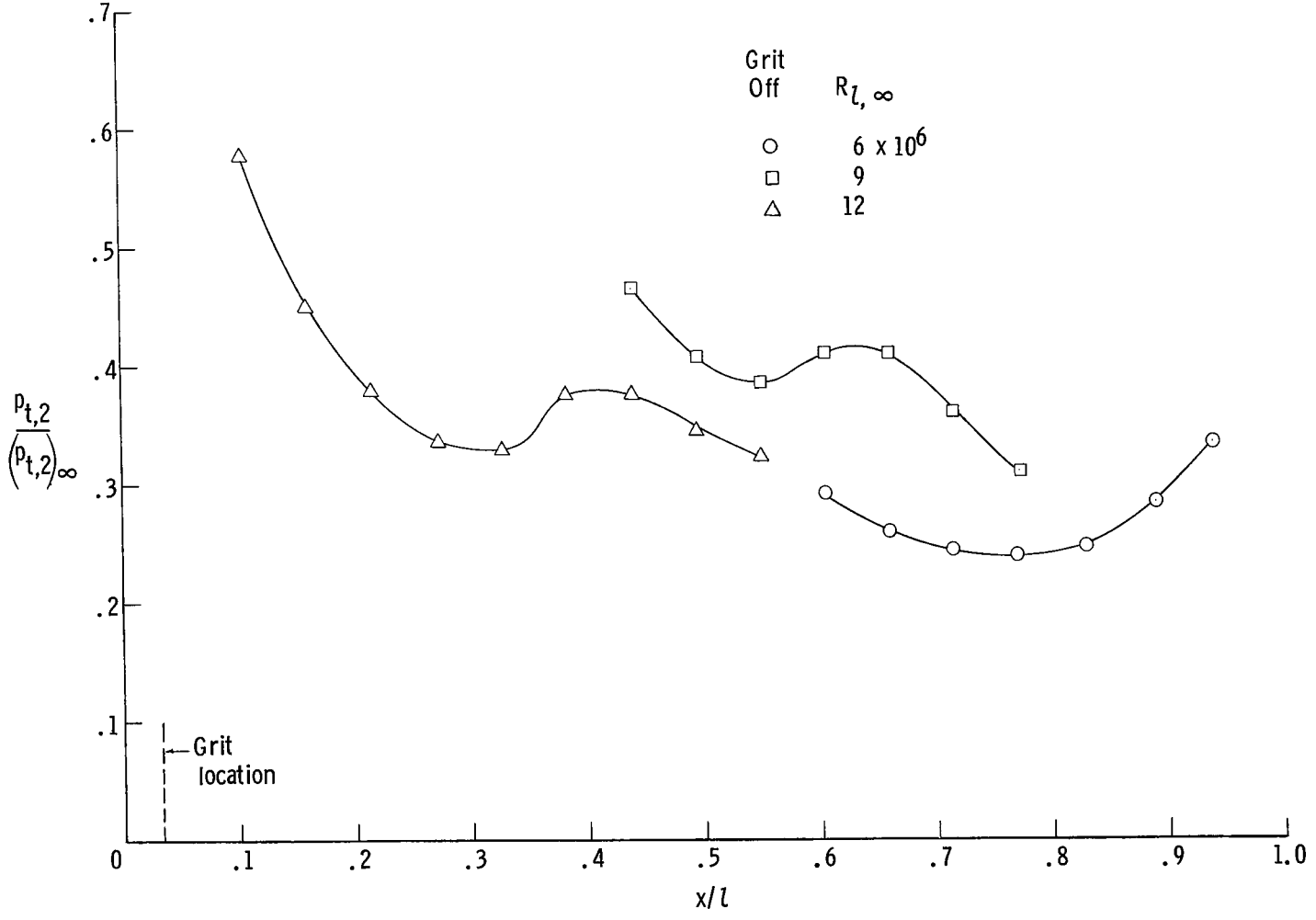

(a) Model A; $M_\infty = 2.00$.

Figure 6.- Longitudinal impact-pressure distribution at $y = 0.0254$ cm.

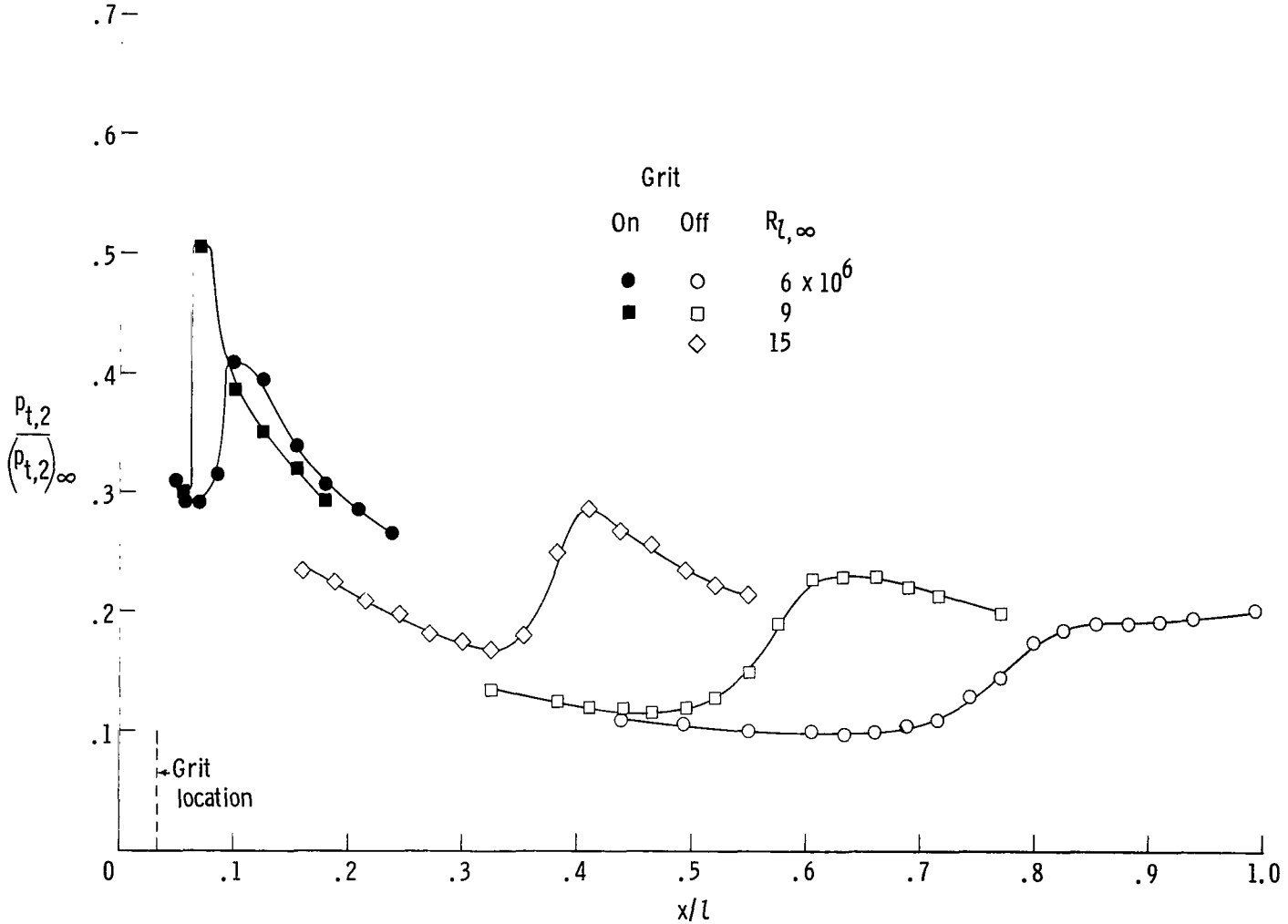

(b) Model A; $M_\infty = 2.75$.

Figure 6.- Continued.

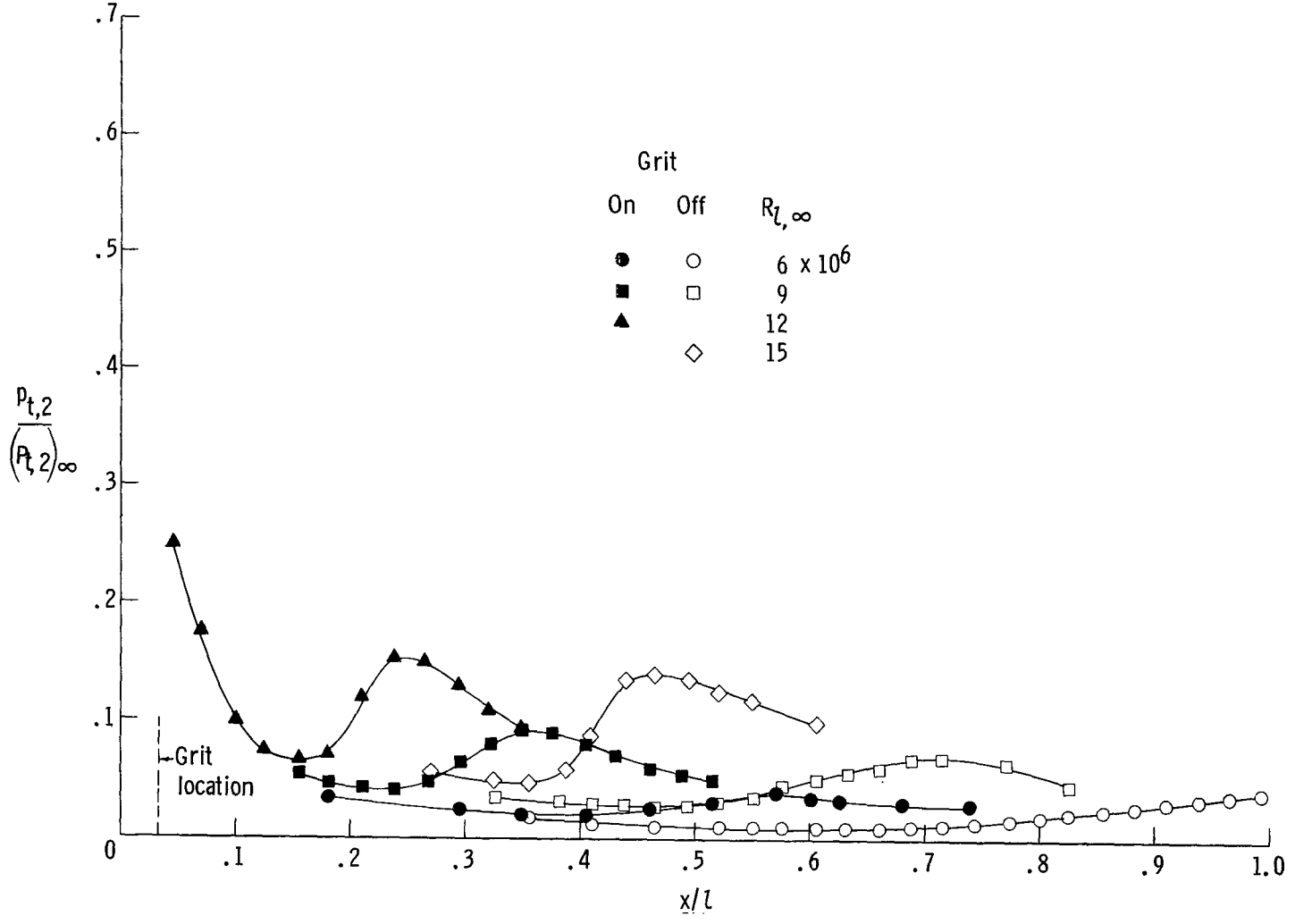

(c) Model A; $M_\infty = 4.63$.

Figure 6.- Continued.

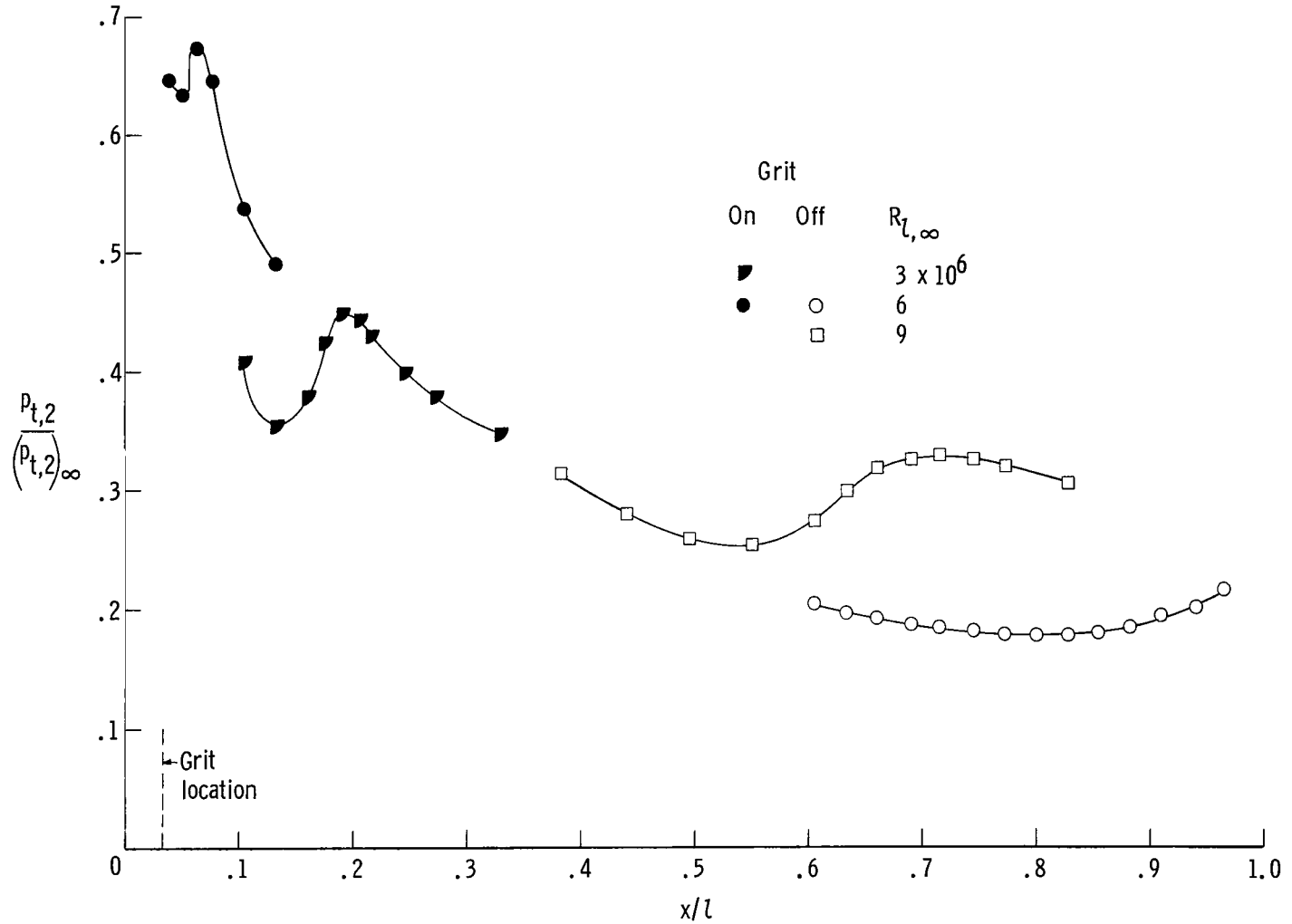

(d) Model B; $M_\infty = 2.00$.

Figure 6.- Continued.

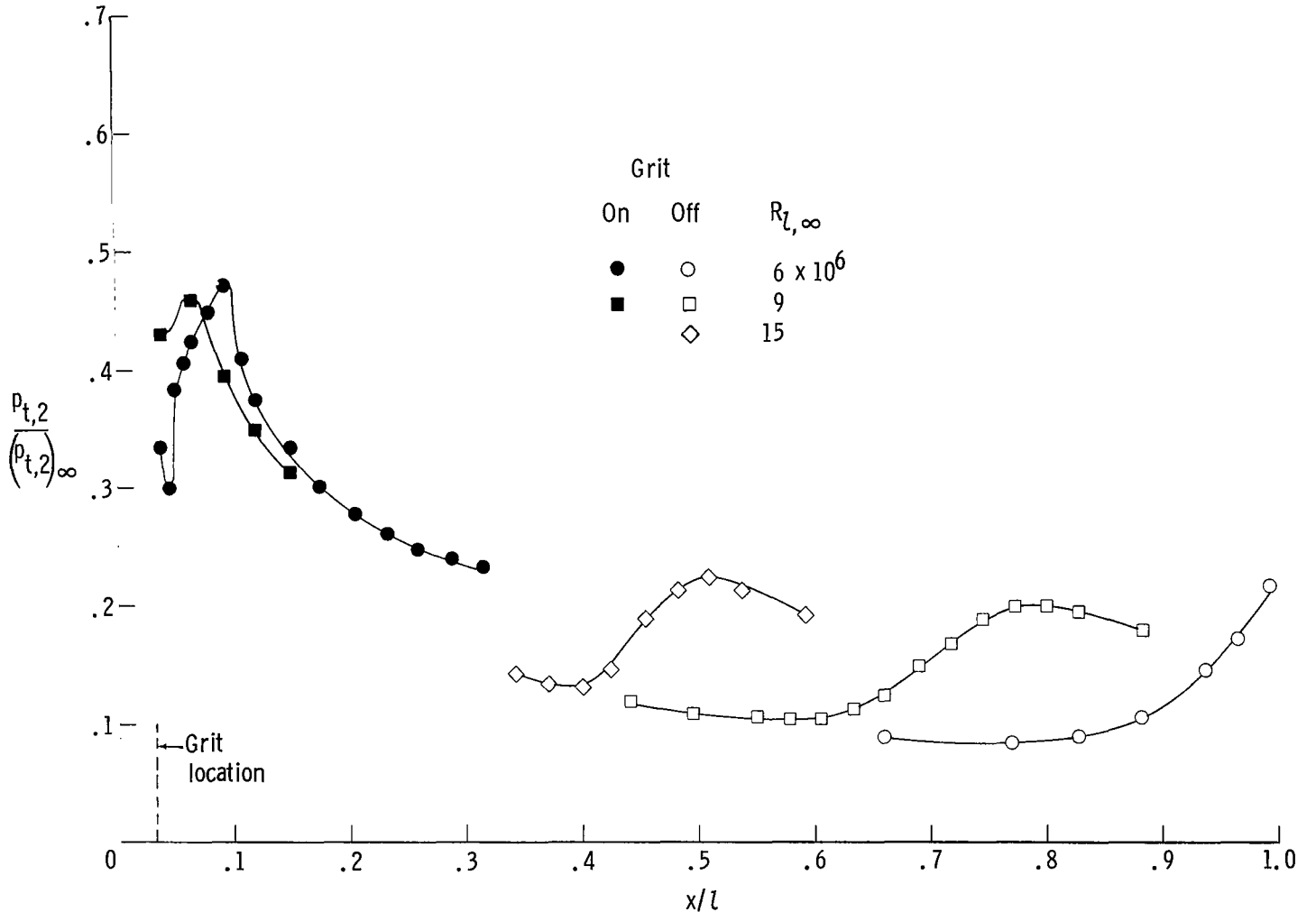

(e) Model B; $M_\infty = 2.75$.

Figure 6.- Continued.

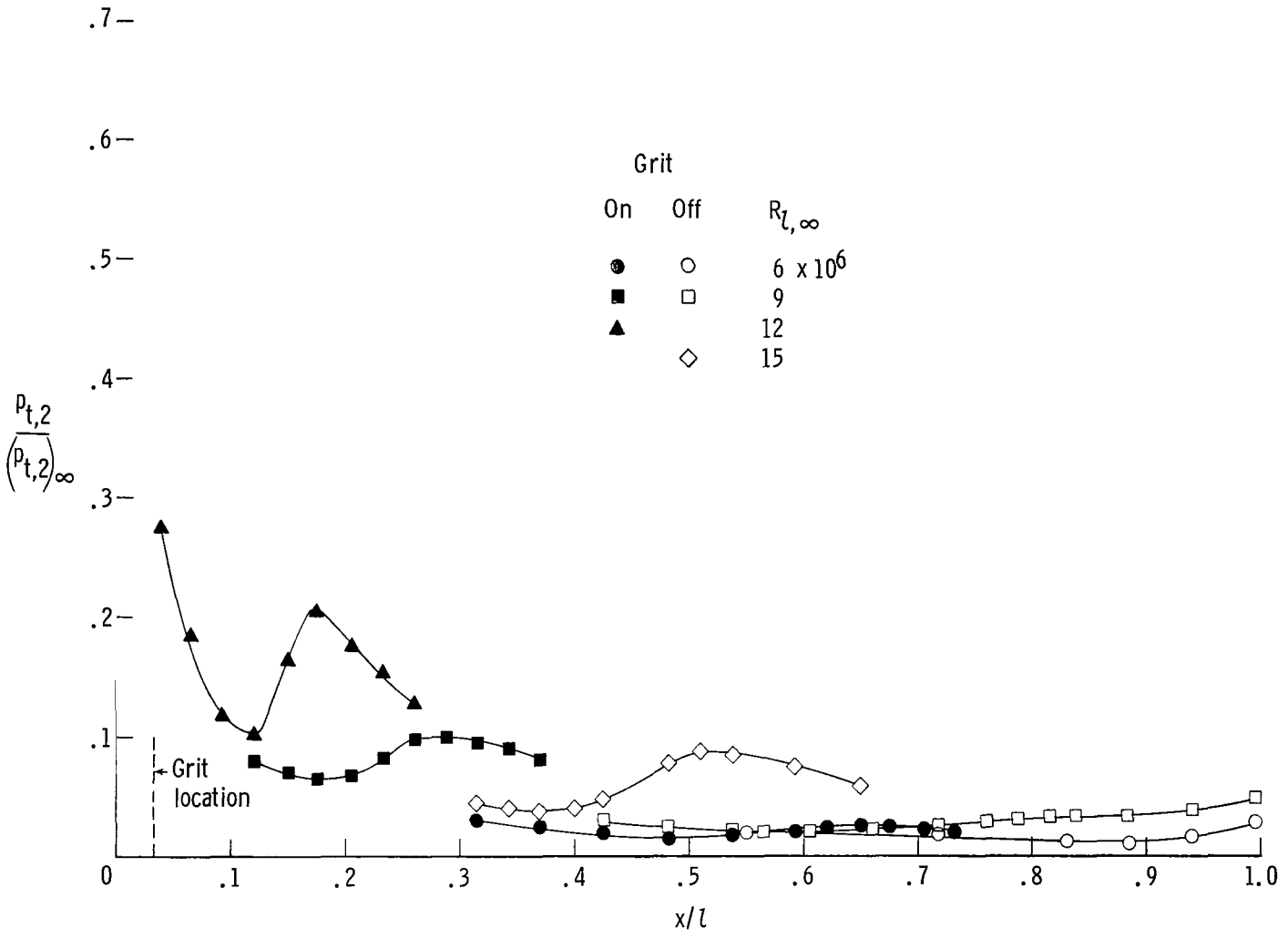

(f) Model B; $M_\infty = 4.63$.

Figure 6.- Continued.

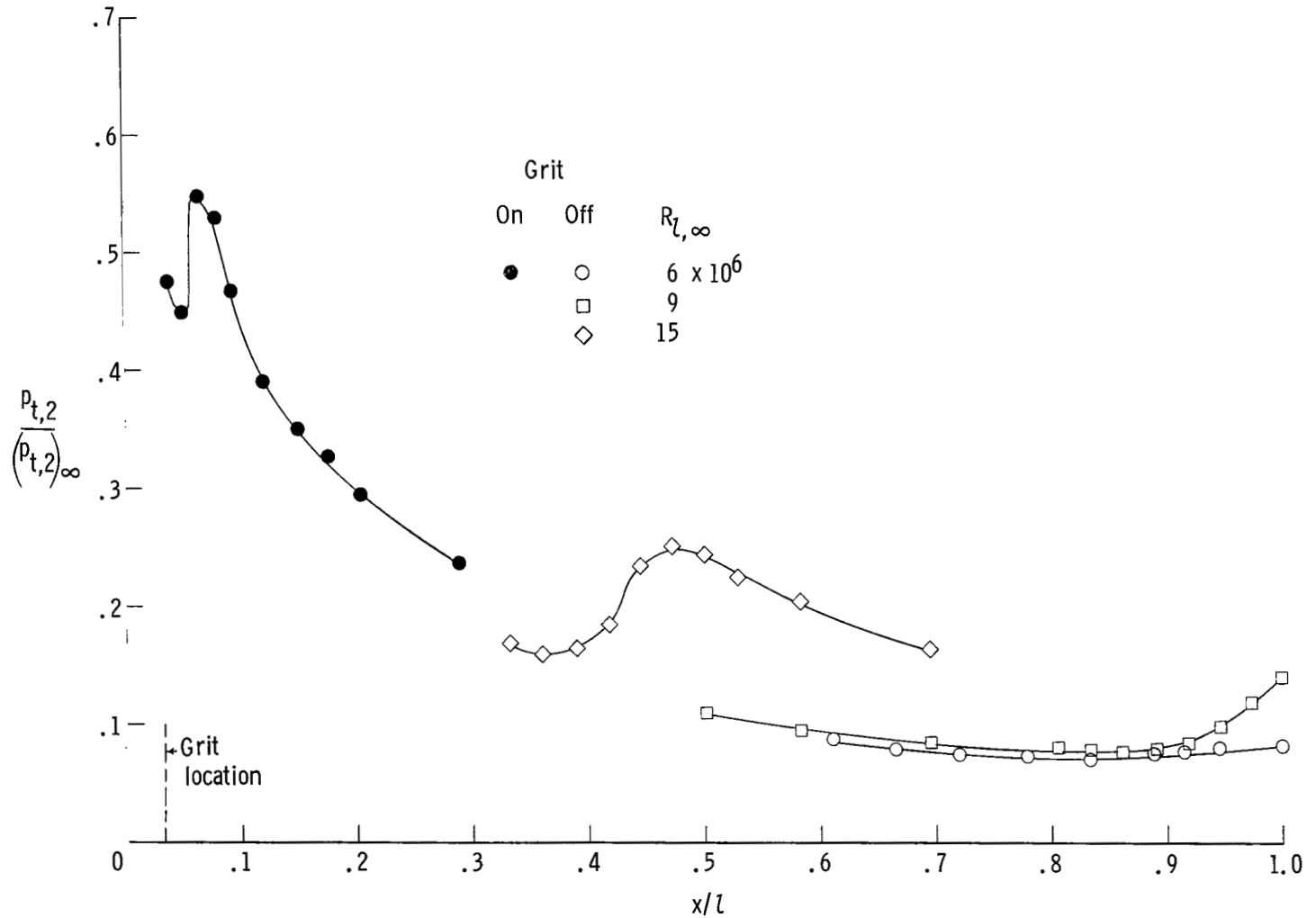

(g) Model C; $M_\infty = 2.75$.

Figure 6.- Continued.

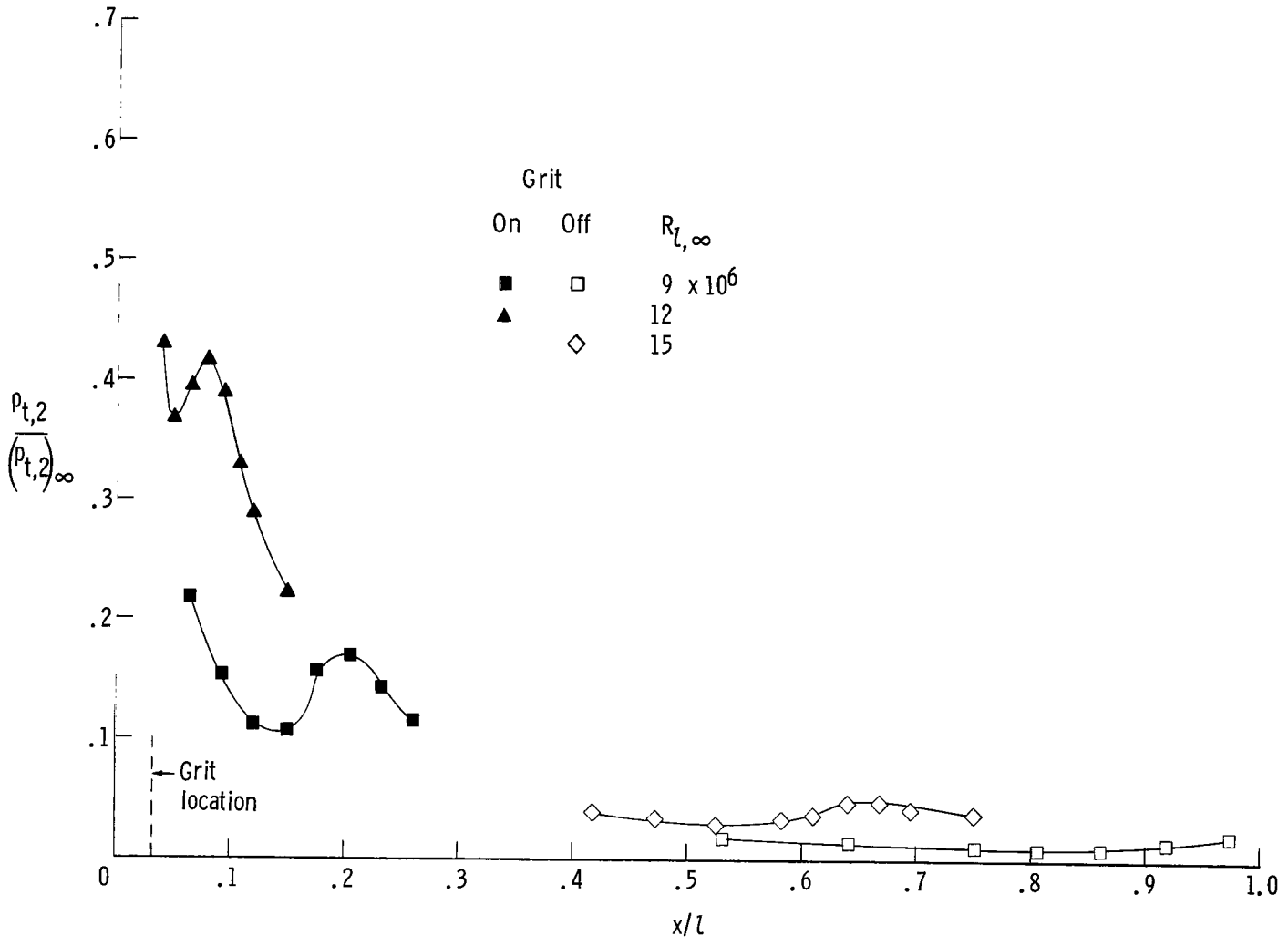

(h) Model C; $M_\infty = 4.63$.

Figure 6.- Concluded.

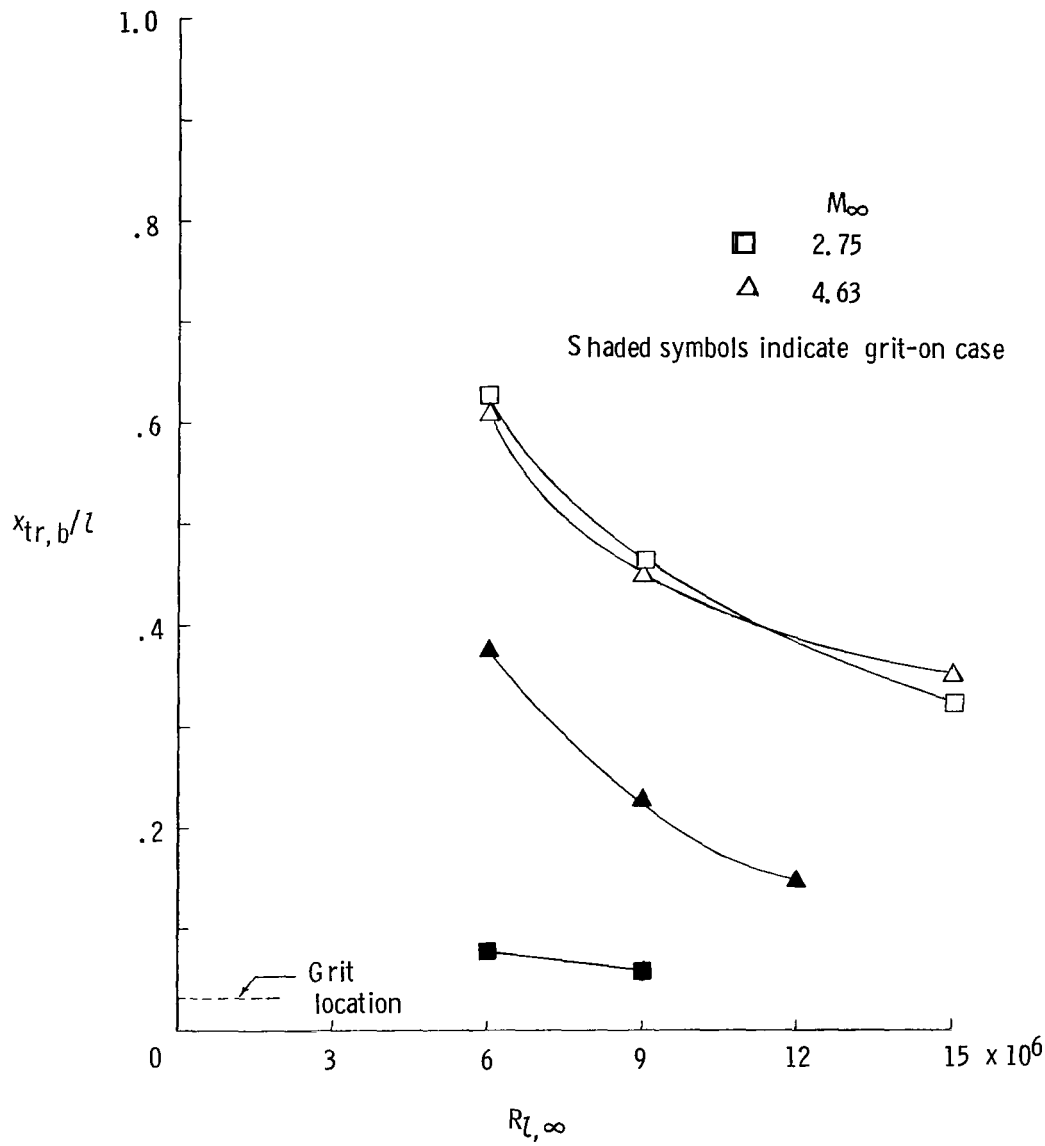

(a) Model A.

Figure 7.- Effect of roughness on transition location for various free-stream Mach numbers and Reynolds numbers.

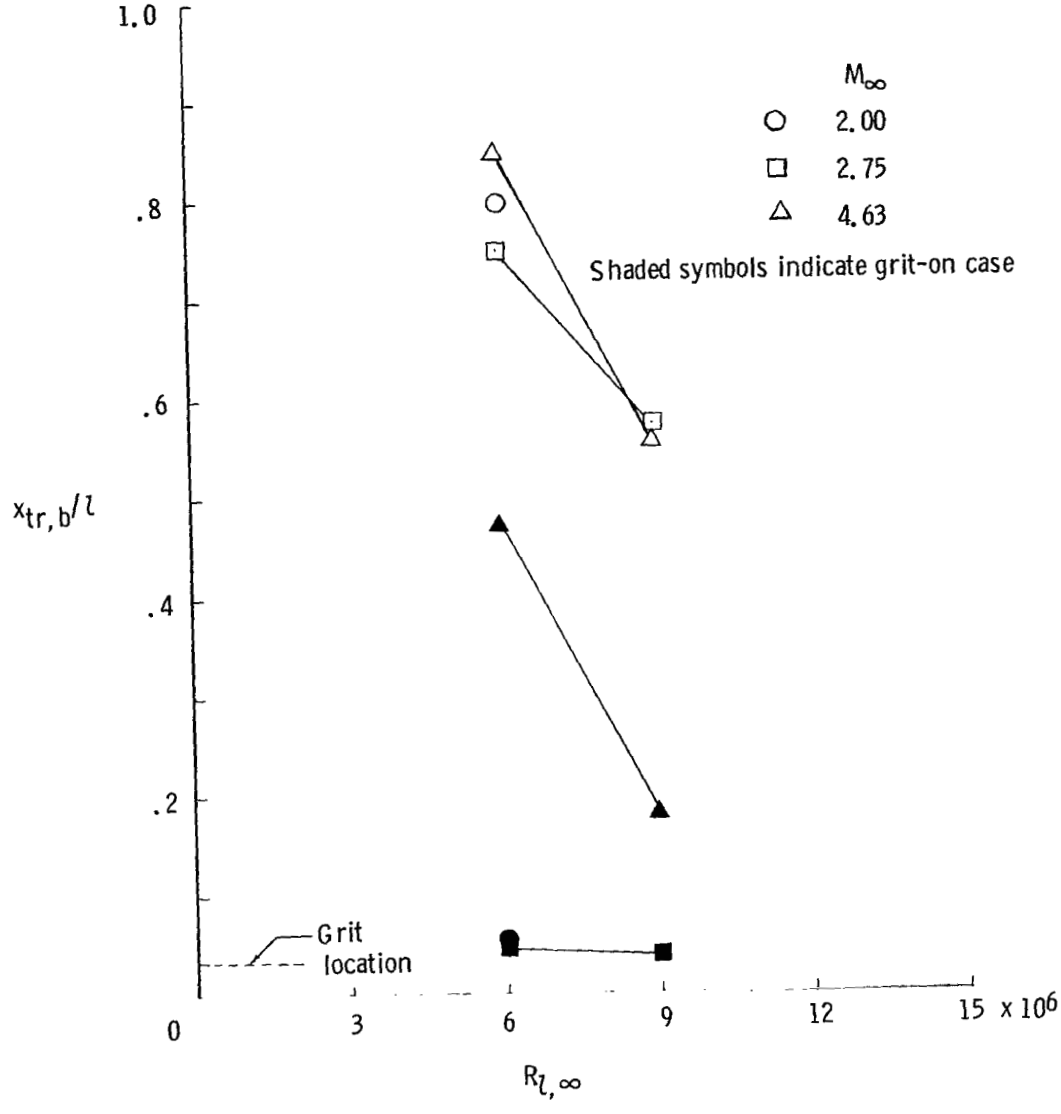

(b) Model B.

Figure 7.- Continued.

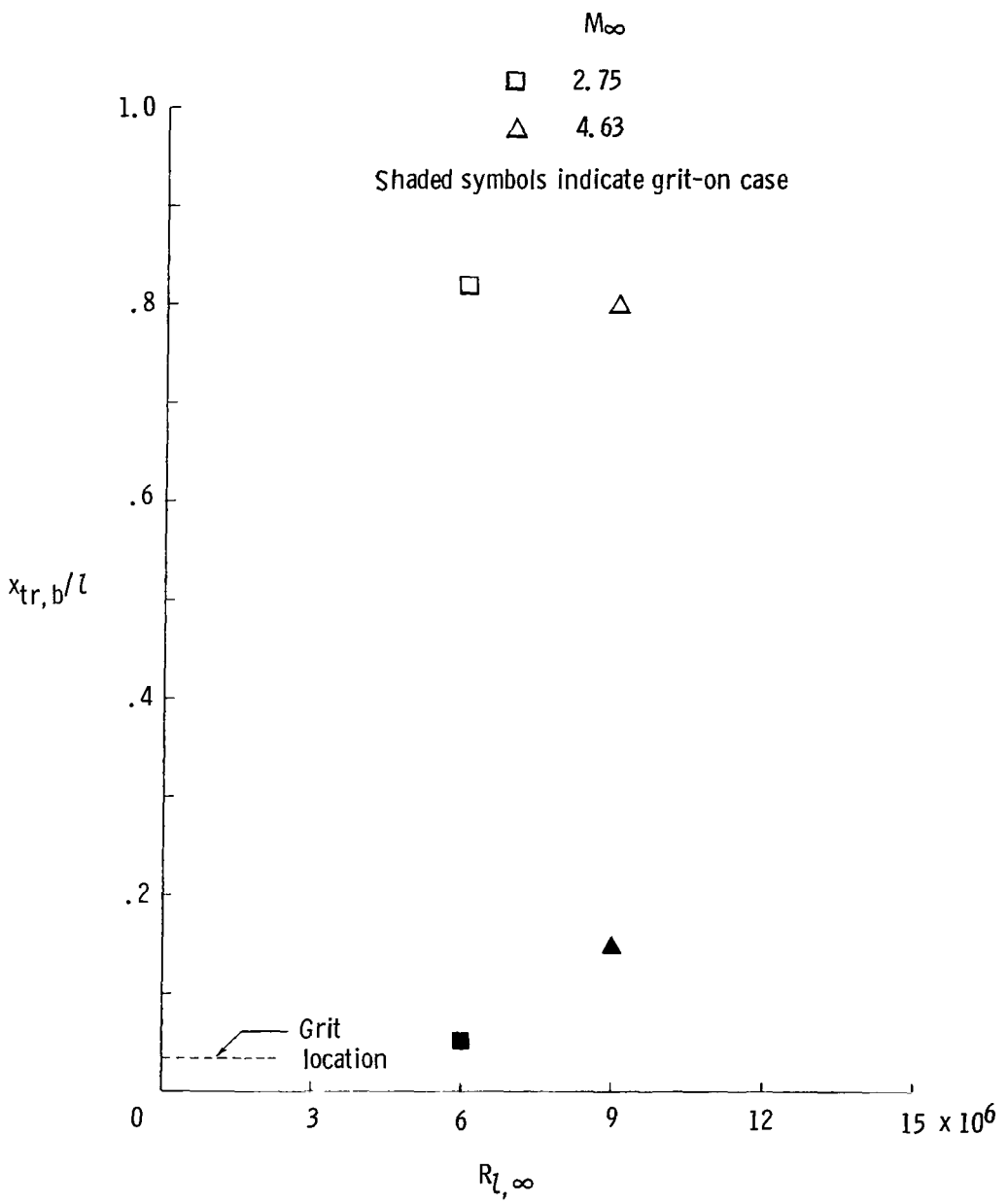

(c) Model C.

Figure 7.- Concluded.

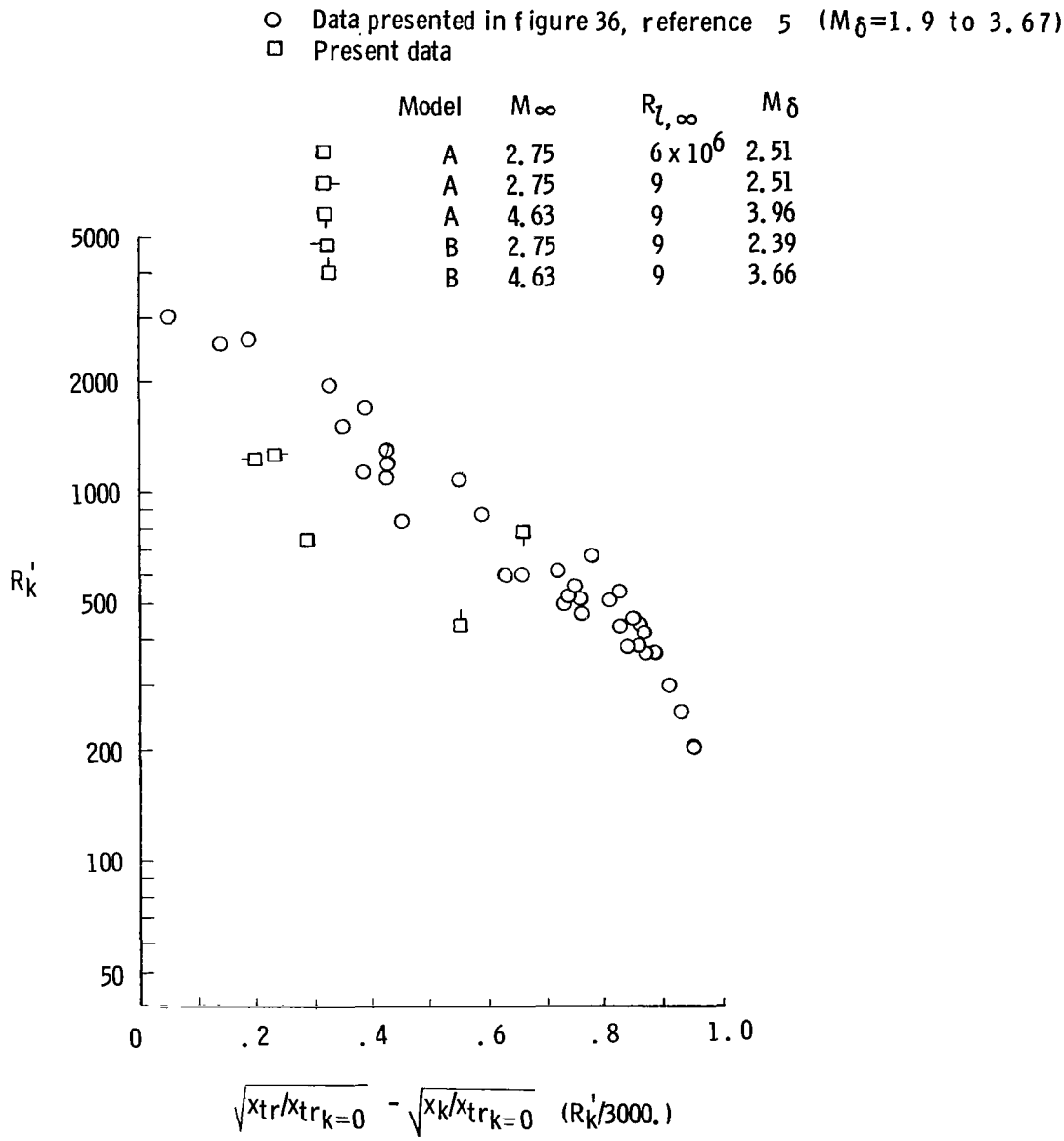

Figure 8.- Comparison of present data with that of figure 36 of reference 5.

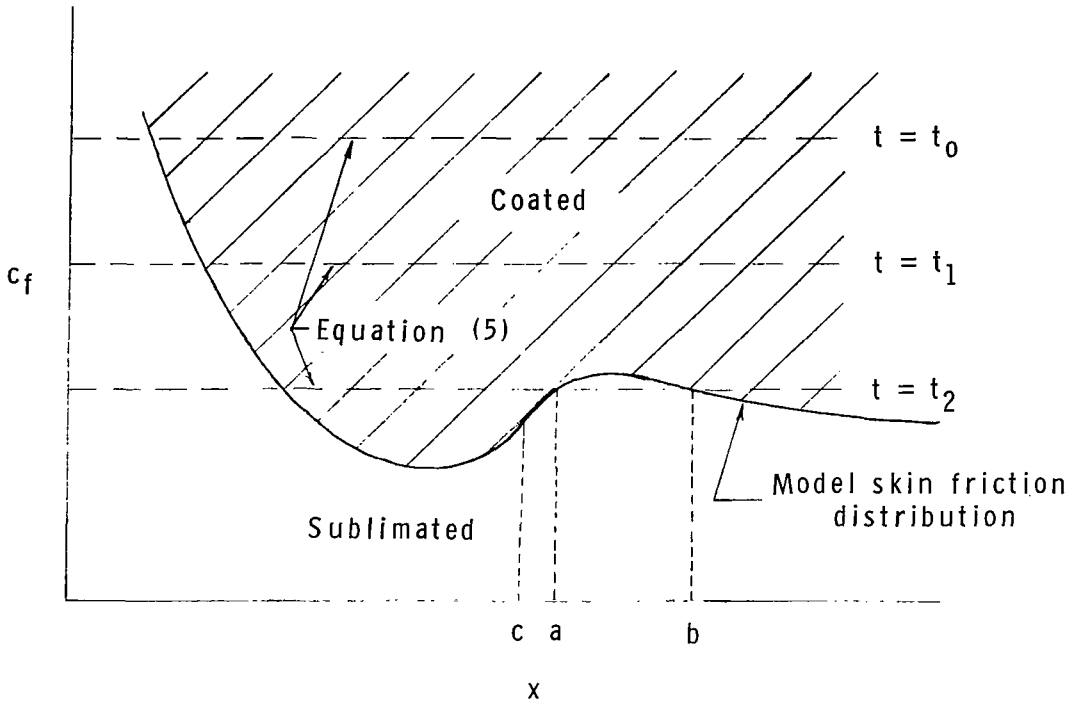

Figure 9.- Schematic of sublimation visualization with velocity distribution assumed constant.

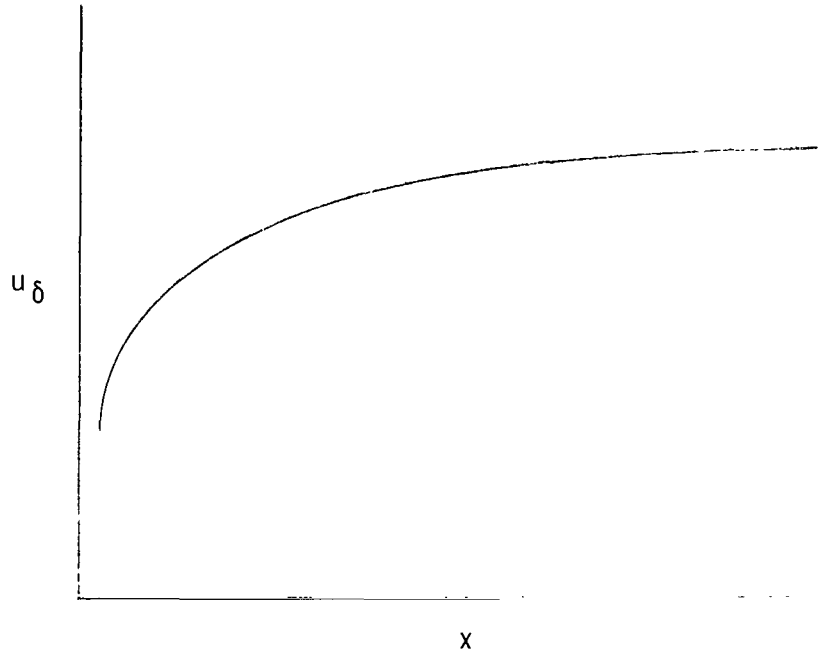

Figure 10.- Variation of local velocity along model.

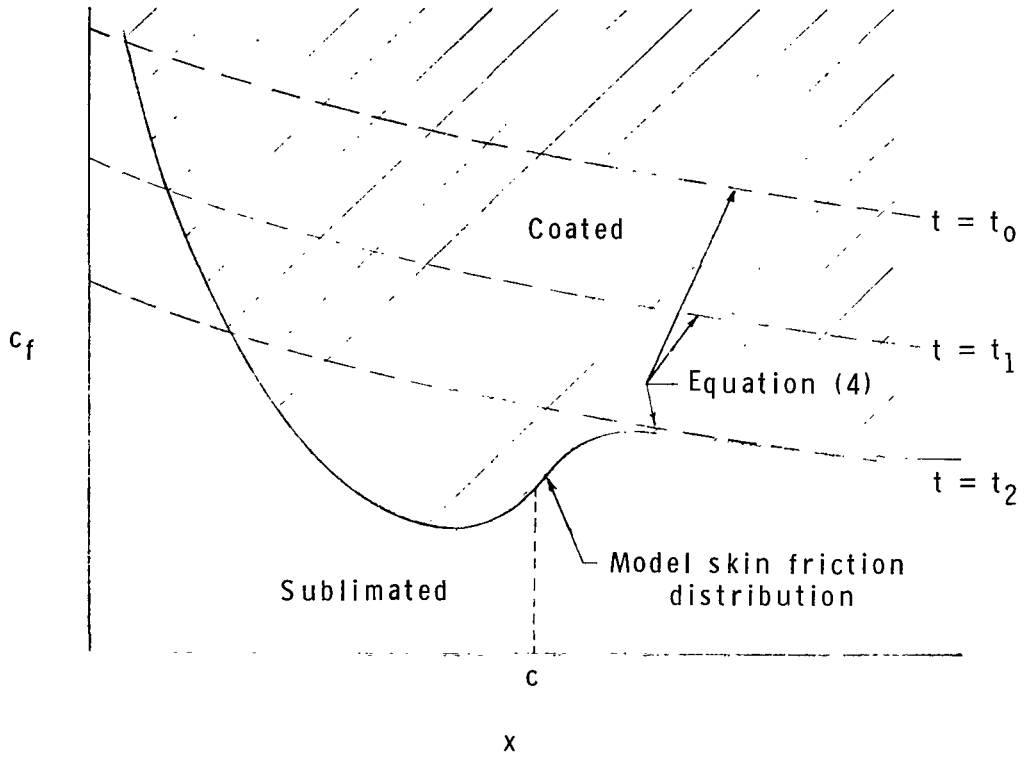

Figure 11.- Schematic of sublimation visualization with variable local velocity.

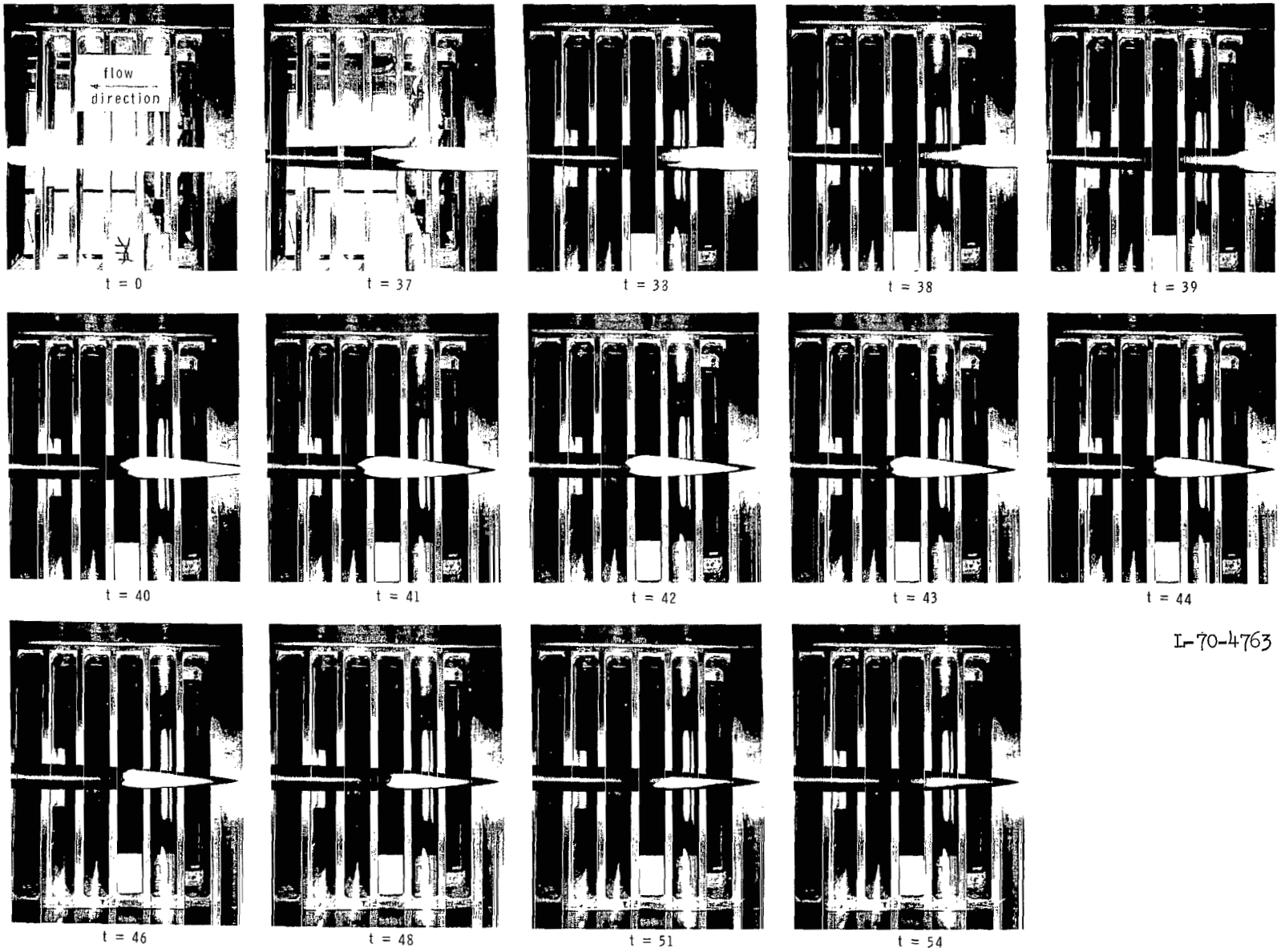

L-70-4763

(a) Model A, grit off; $M_\infty = 4.63$; $R_{l,\infty} = 15 \times 10^6$.

Figure 12.- Sublimation test photograph sequence. Flow from right to left; time t is in minutes.

L-70-4764

(b) Model B, grit on; $M_\infty = 4.63$; $R_{l,\infty} = 9 \times 10^6$.

Figure 12.- Concluded.

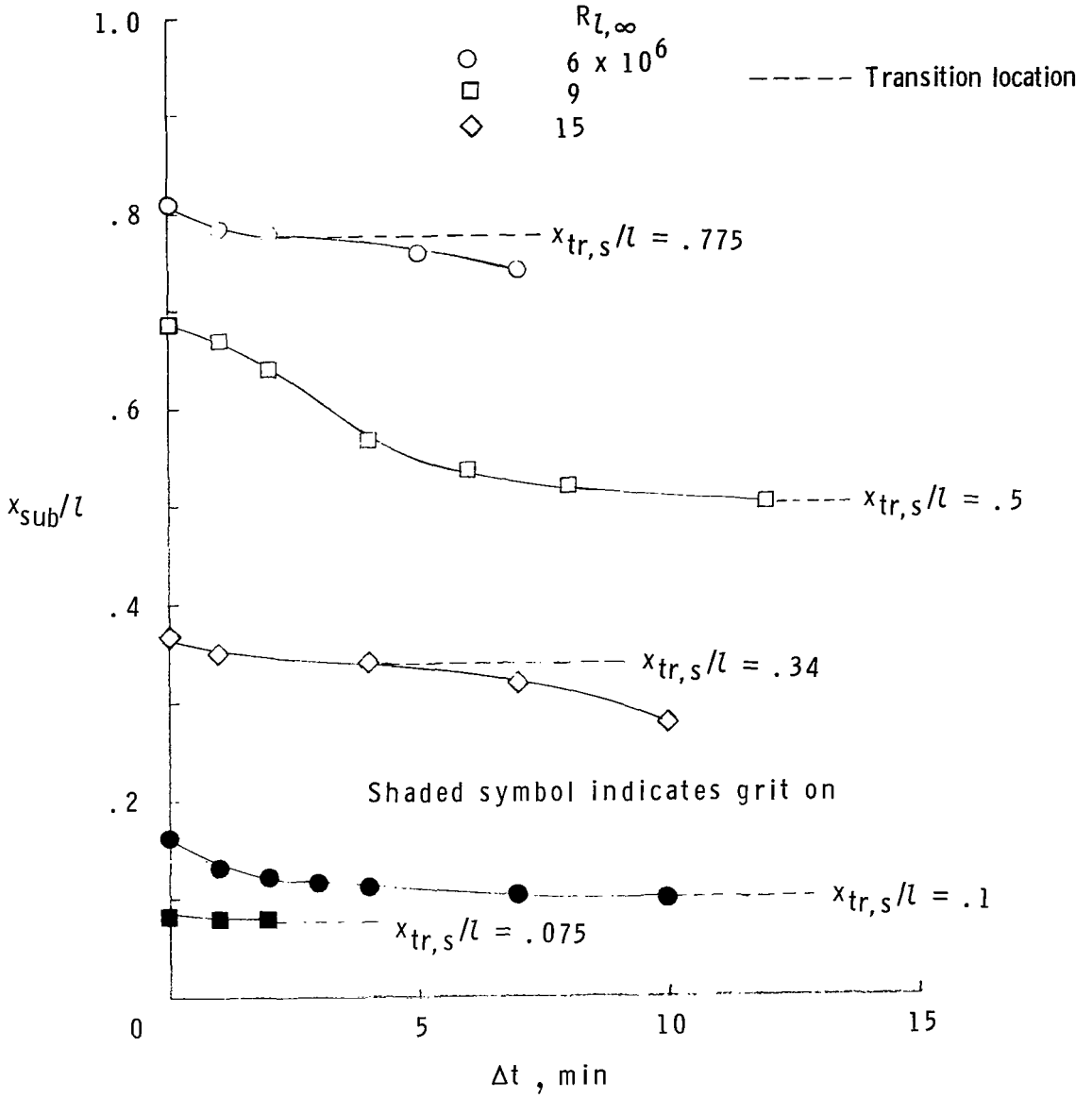

(a) Model A; M_∞ = 2.75.

Figure 13.- Sublimation progression along models as a function of time from the first picture after flow was established.

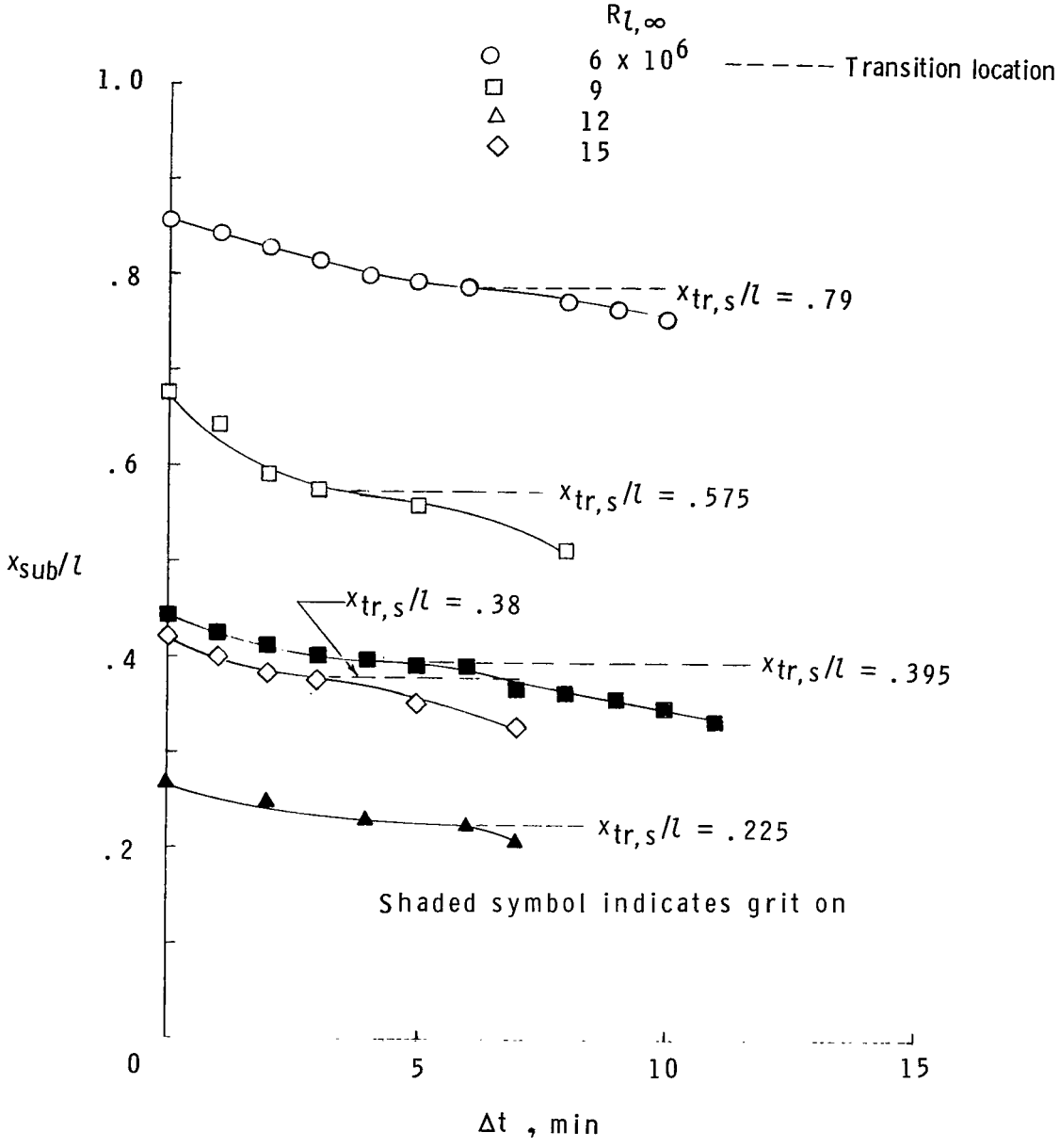

(b) Model A; $M_\infty = 4.63$.

Figure 13.- Continued.

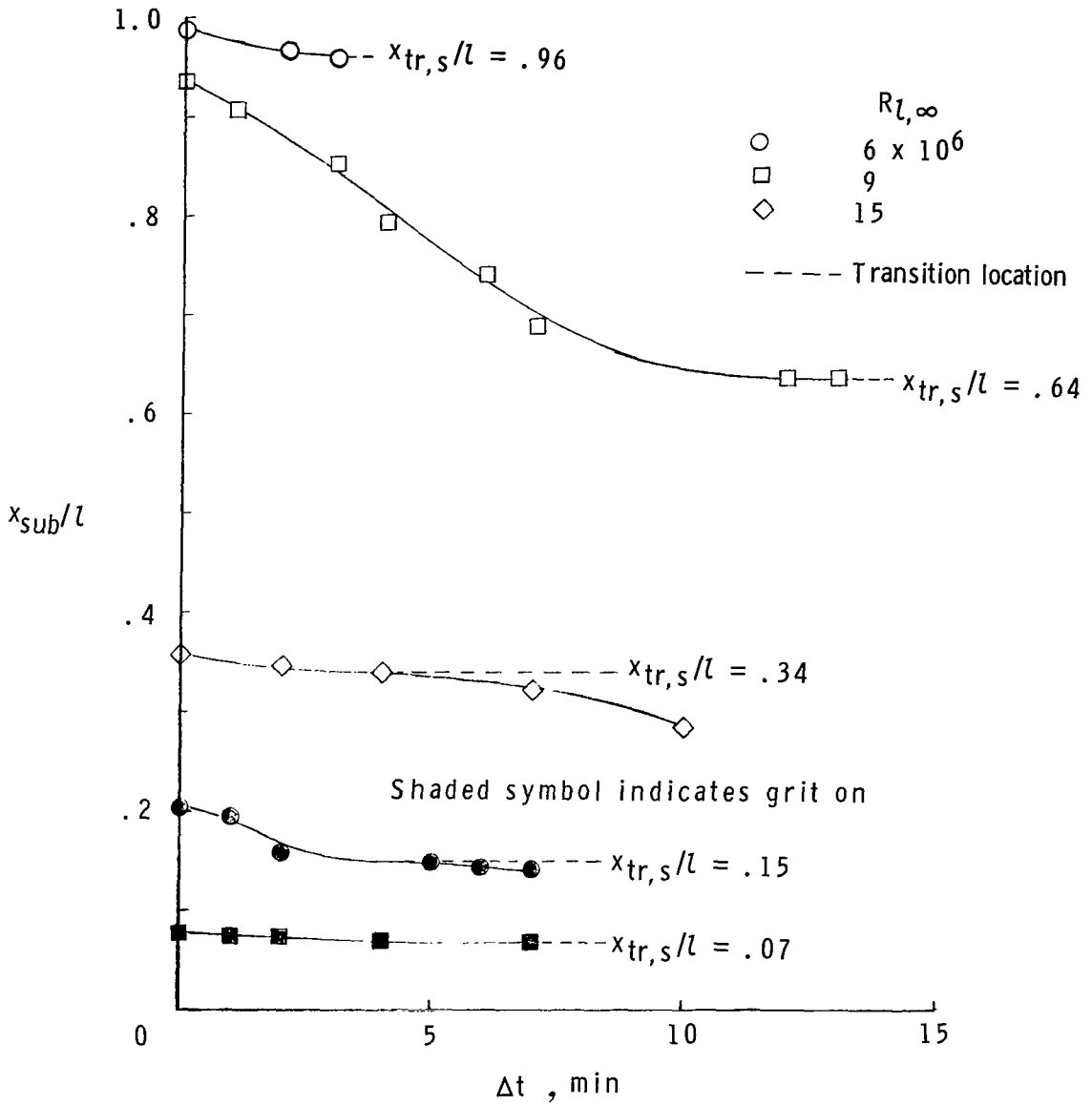

(c) Model B; $M_\infty = 2.75$.

Figure 13.- Continued.

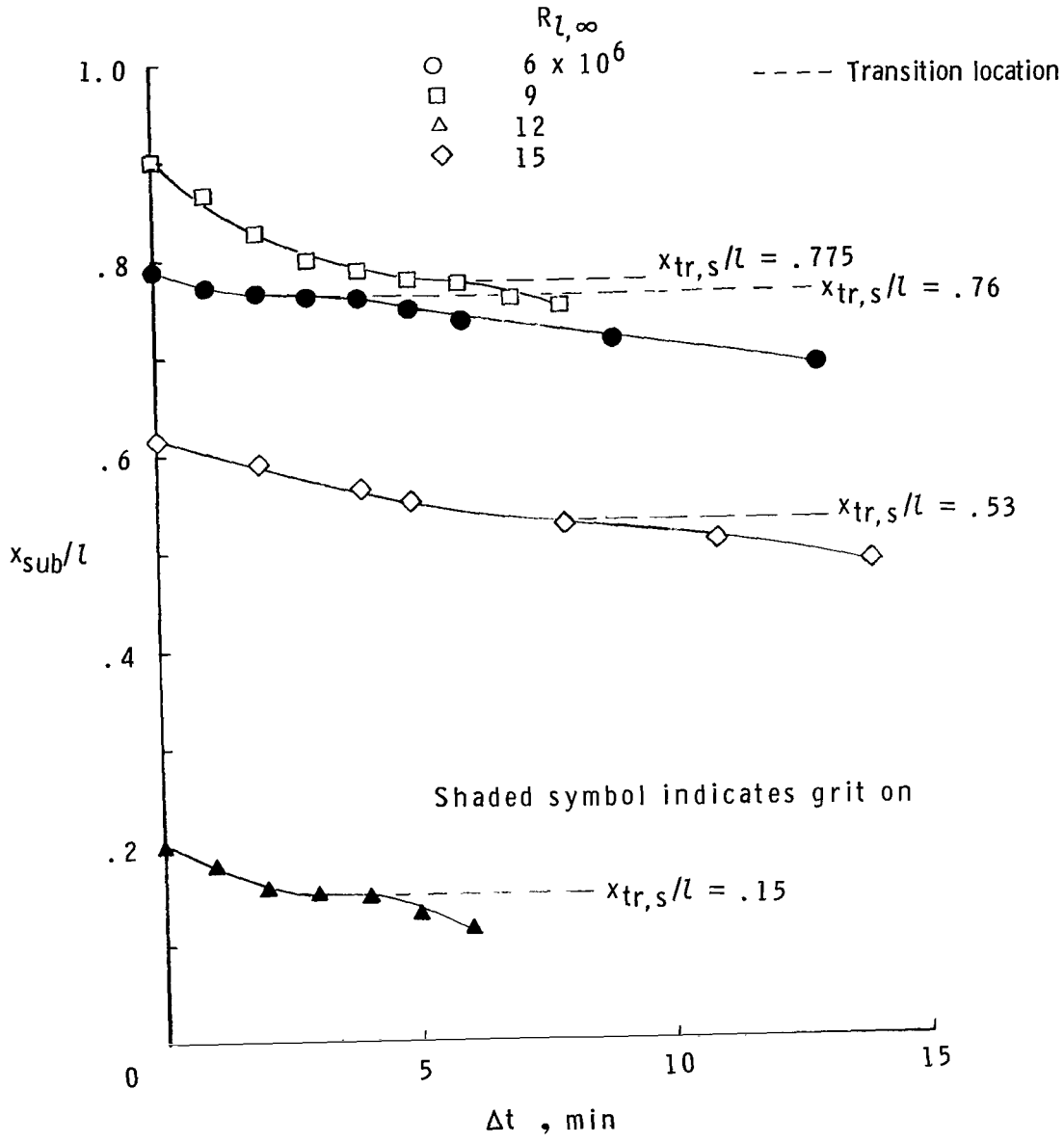

(d) Model B; $M_\infty = 4.63$.

Figure 13.- Continued.

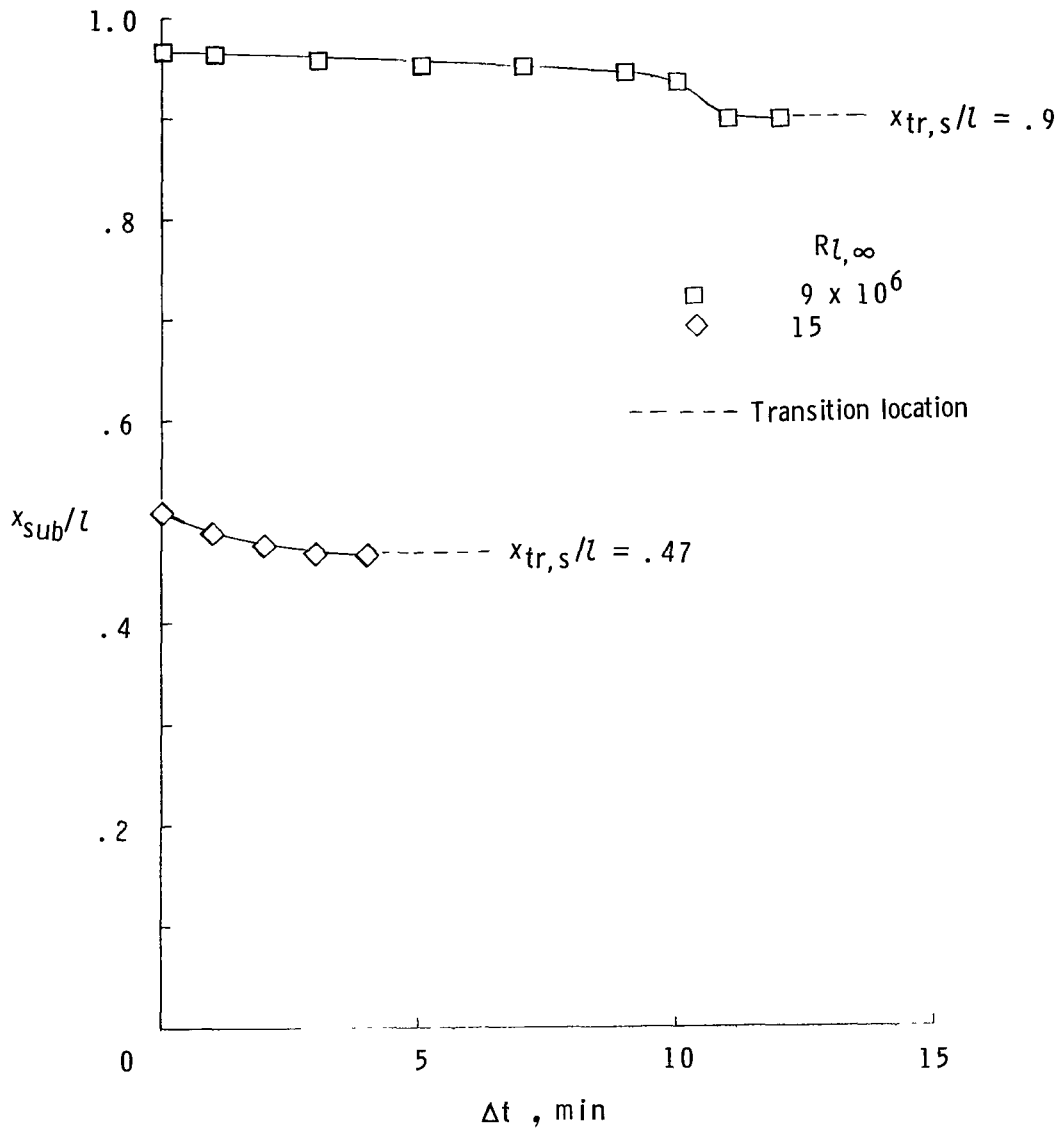

(e) Model C; M_∞ = 2.75.

Figure 13.- Continued.

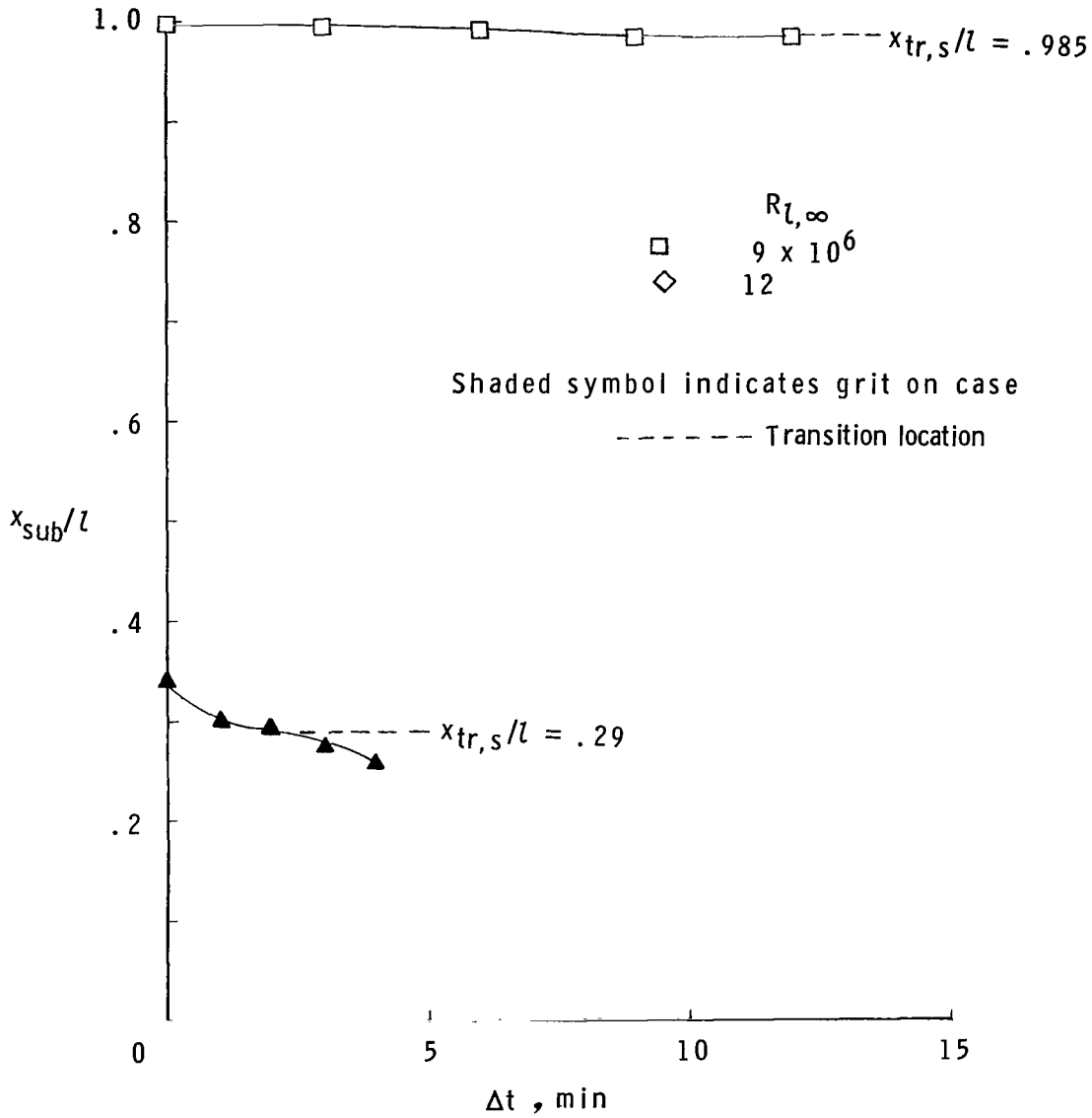

(f) Model C; $M_\infty = 4.63$.

Figure 13.- Concluded.

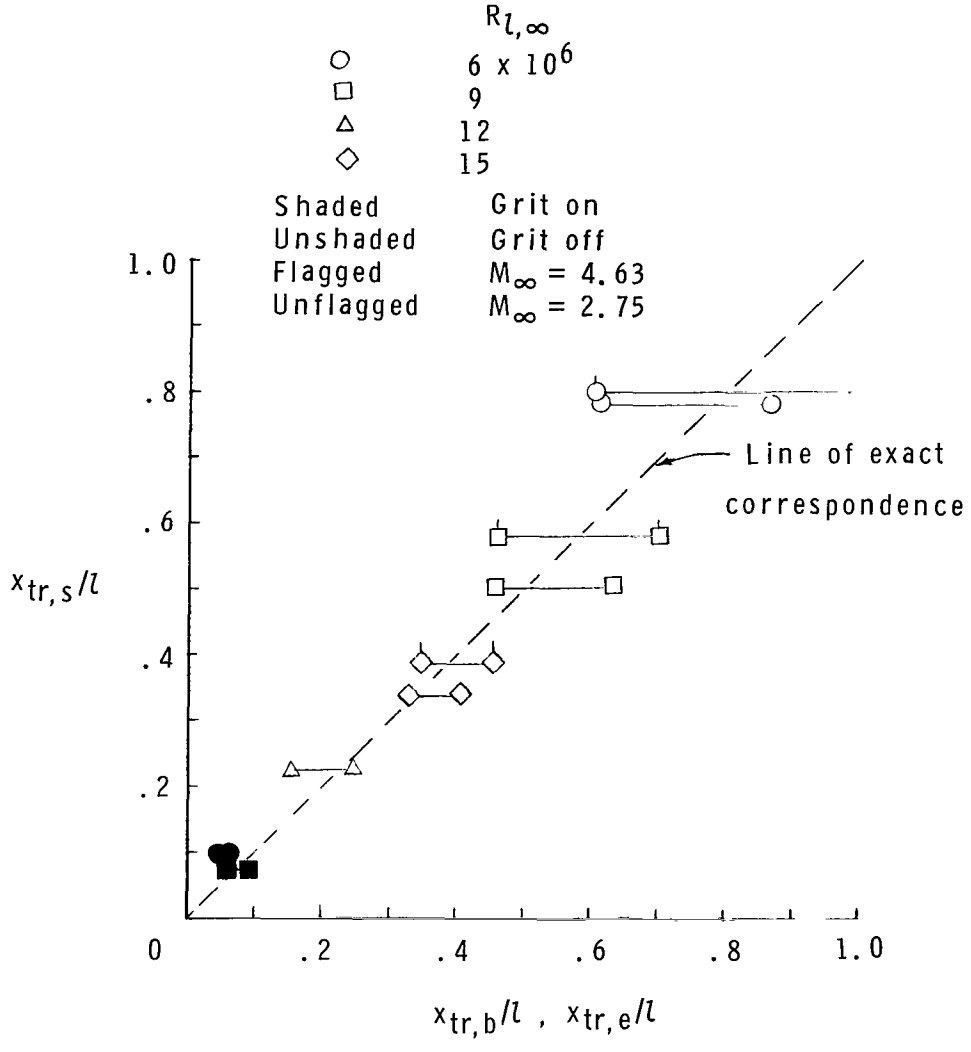

(a) Model A.

Figure 14.- Correlation of sublimation and impact-pressure results.

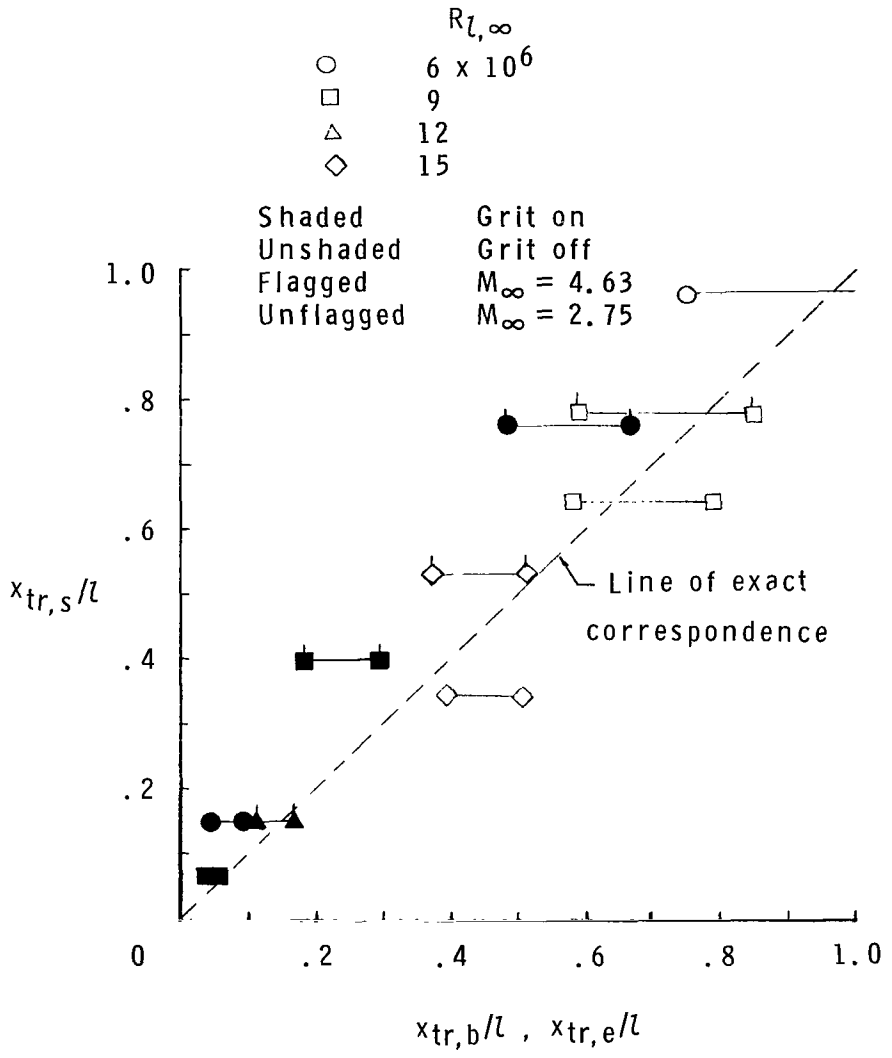

(b) Model B.

Figure 14.- Continued.

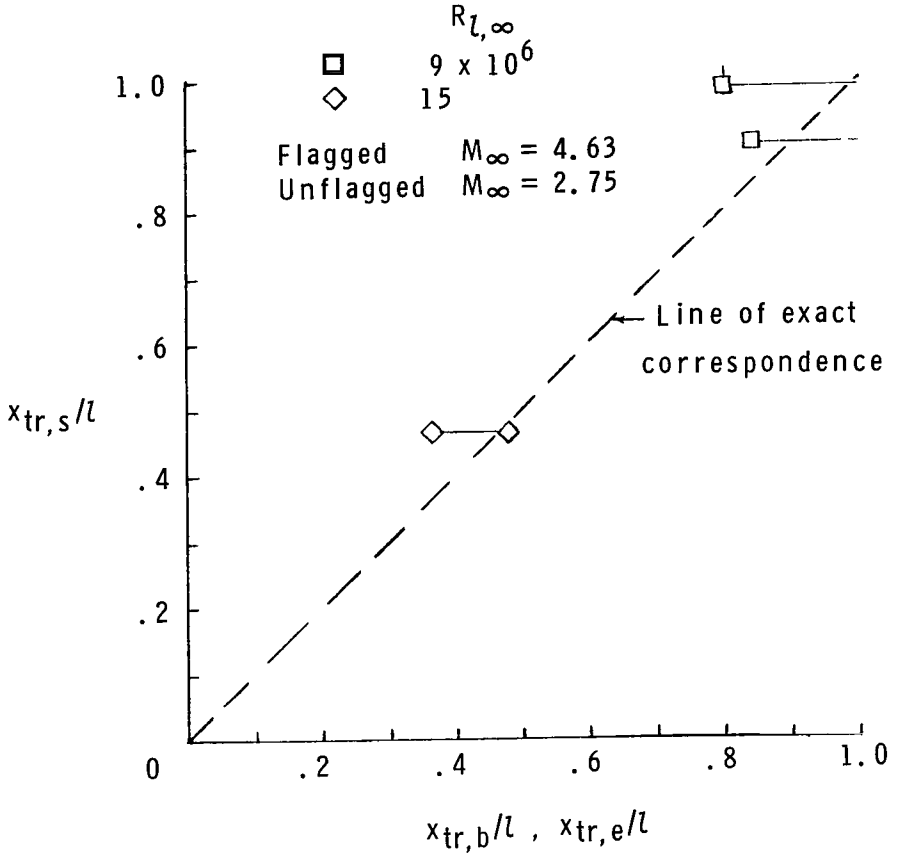

(c) Model C.

Figure 14.- Concluded.

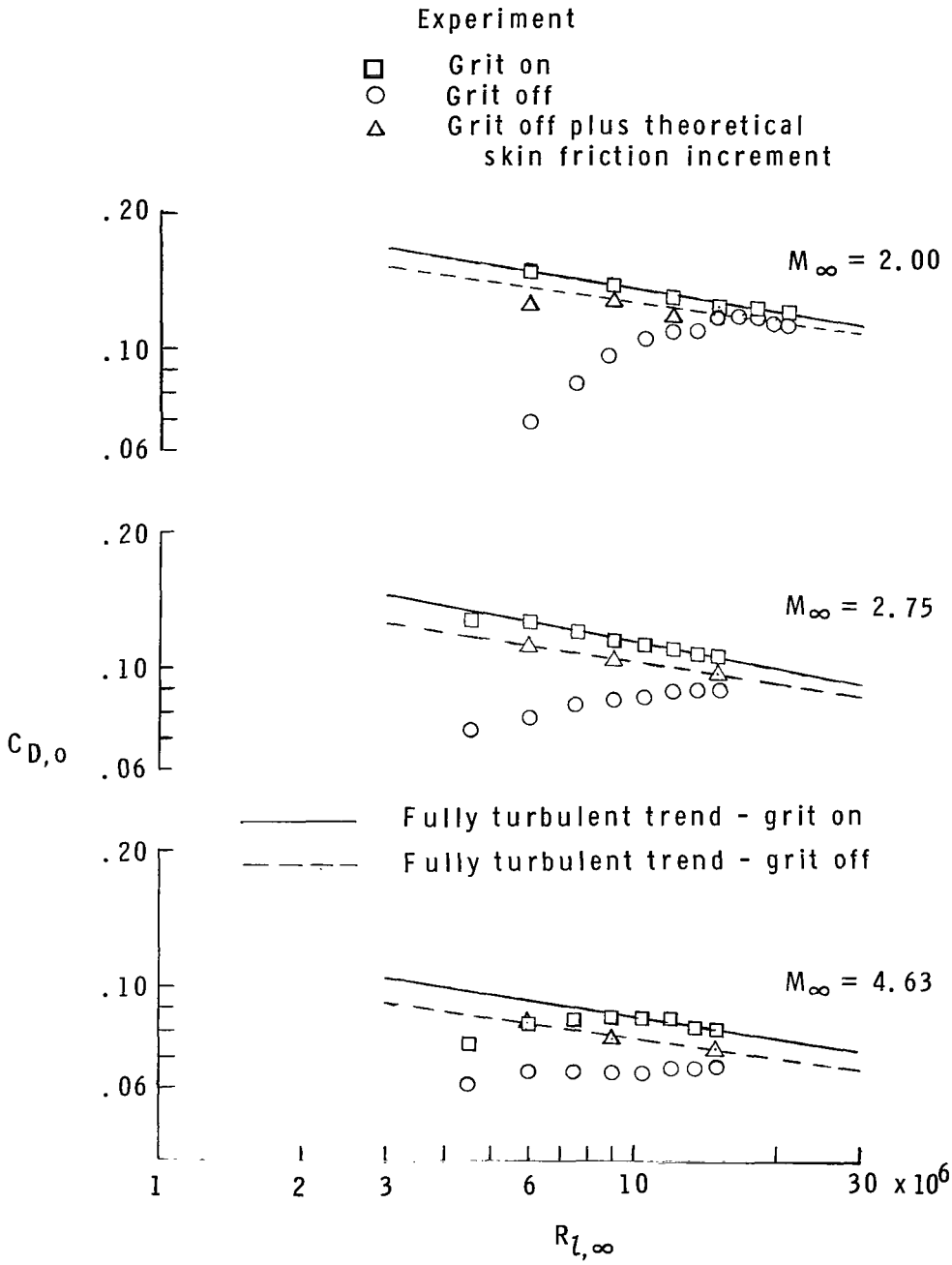

(a) Model A.

Figure 15.- Variation of drag coefficient with free-stream Reynolds number.

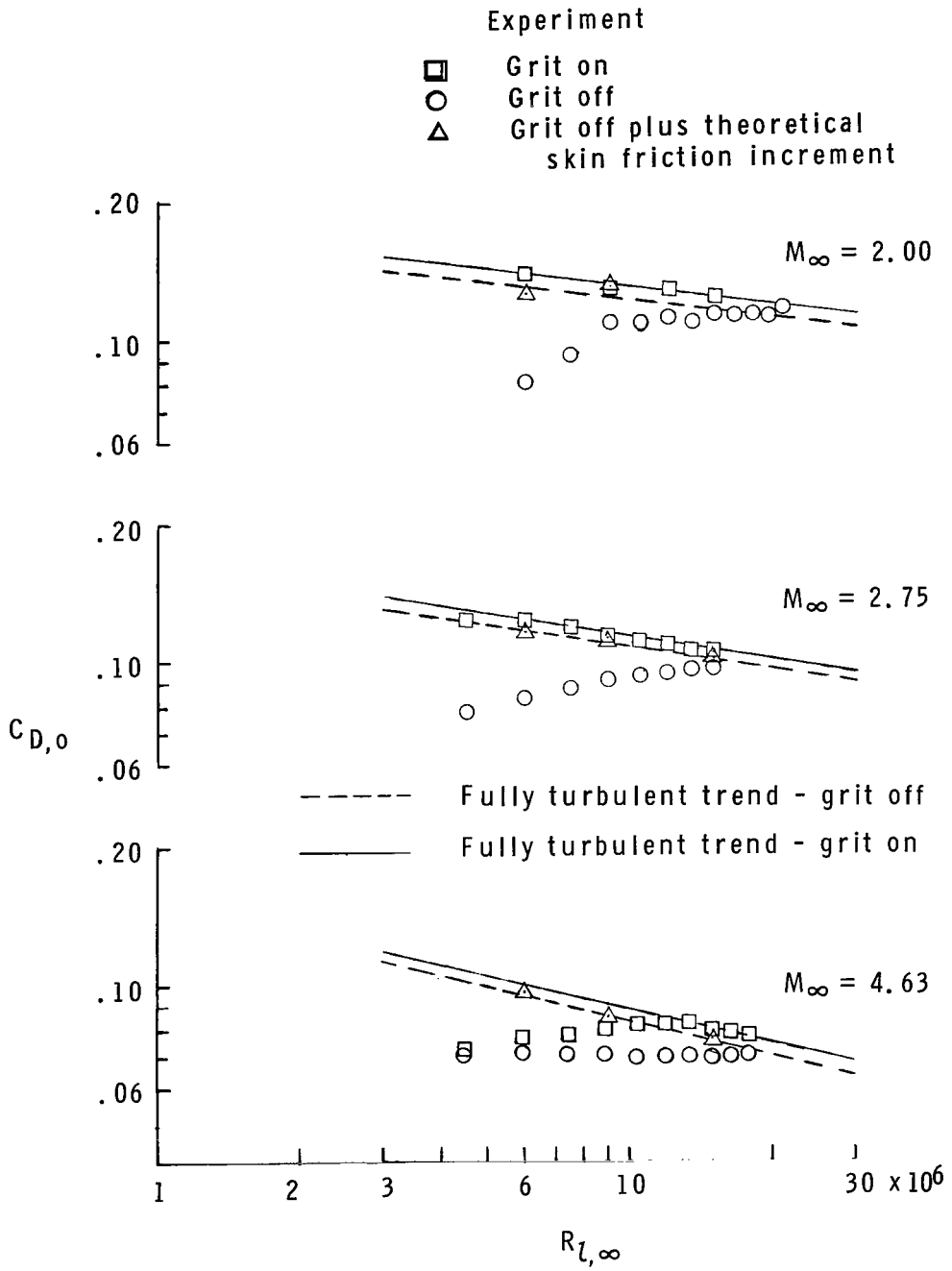

(b) Model B.

Figure 15.- Continued.

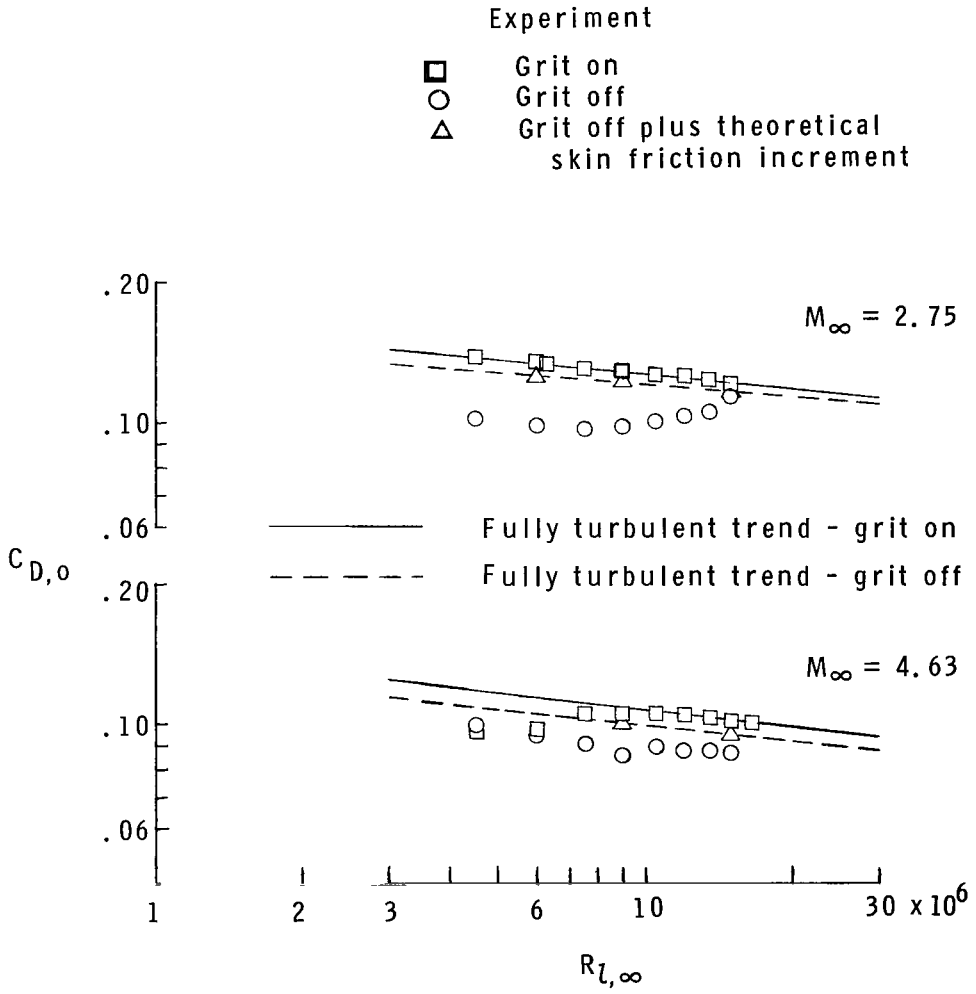

(c) Model C.

Figure 15.- Concluded.

"The aeronautical and space activities of the United States shall be conducted so as to contribute . . . to the expansion of human knowledge of phenomena in the atmosphere and space. The Administration shall provide for the widest practicable and appropriate dissemination of information concerning its activities and the results thereof."

—NATIONAL AERONAUTICS AND SPACE ACT OF 1958

NASA SCIENTIFIC AND TECHNICAL PUBLICATIONS

TECHNICAL REPORTS: Scientific and technical information considered important, complete, and a lasting contribution to existing knowledge.

TECHNICAL NOTES: Information less broad in scope but nevertheless of importance as a contribution to existing knowledge.

TECHNICAL MEMORANDUMS: Information receiving limited distribution because of preliminary data, security classification, or other reasons.

CONTRACTOR REPORTS: Scientific and technical information generated under a NASA contract or grant and considered an important contribution to existing knowledge.

TECHNICAL TRANSLATIONS: Information published in a foreign language considered to merit NASA distribution in English.

SPECIAL PUBLICATIONS: Information derived from or of value to NASA activities. Publications include conference proceedings, monographs, data compilations, handbooks, sourcebooks, and special bibliographies.

TECHNOLOGY UTILIZATION PUBLICATIONS: Information on technology used by NASA that may be of particular interest in commercial and other non-aerospace applications. Publications include Tech Briefs, Technology Utilization Reports and Notes, and Technology Surveys.

Details on the availability of these publications may be obtained from:

SCIENTIFIC AND TECHNICAL INFORMATION DIVISION

NATIONAL AERONAUTICS AND SPACE ADMINISTRATION

Washington, D.C. 20546